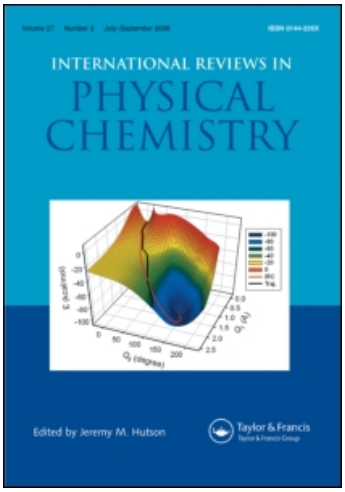

International Reviews in Physical Chemistry
Publication details, including instructions for authors and subscription information:
http://www.informaworld.com/smpp/title~content=t713724383

Generation and characterization of aerosols

C. N. Davies[a]
[a] Pilcox Hall, Essex, England

To cite this Article Davies, C. N.(1987) 'Generation and characterization of aerosols', International Reviews in Physical Chemistry, 6: 2, 143 — 194
To link to this Article: DOI: 10.1080/01442358709353404
URL: http://dx.doi.org/10.1080/01442358709353404

INTERNATIONAL REVIEWS IN PHYSICAL CHEMISTRY, 1987, VOL.6, NO. 2, 143–194

Generation and characterization of aerosols

by C. N. DAVIES
Pilcox Hall, Tendring, Essex CO16 0DP, England

Section 1, the nature of aerosols, explains their instability, their action on light, the mutual influence of particles, the drag of particles and their size and shape. Sections 2, 3 and 4 are concerned with atmospheric aerosols.

Section 2 is about measuring the aerosols of the atmosphere and describes condensation nucleus counters and the way in which the size of particles initiating condensation depends on supersaturation. Visual range and atmospheric opacity are discussed, the latter having possible effects on climate.

Section 3 discusses the generation of aerosols in the atmosphere, including volcanoes, desert dust, trees and human sources, particularly combustion. Size distributions of the atmospheric aerosol are the subject of Section 4, including impactor sampling.

The rest of the article is devoted to laboratory aerosols and fundamental aerosol science: Section 5, aerosol generators; Section 6, particle size and size distributions; Section 7, the dynamics of aerosol particles; Section 8, Brownian motion and diffusion; Section 9, coagulation; Section 10, evaporation and condensation; Section 11, compositional analysis, including individual particles.

1. Nature of aerosols

An aerosol is a suspension of fine particles in a gas. Owing to the sedimentation of larger particles under gravity, and the diffusion and coagulation of smaller ones due to Brownian motion, aerosols are inherently unstable. Particles of intermediate size, often around 0·5 μm, have minimal motion relative to the suspending gas so that such aerosols may appear to be relatively stable. In flowing aerosols the inertia of the larger particles may cause them to deviate from the lines of flow which results in loss of particles by impaction on surfaces which confine the flow. Due to molecular attraction aerosol particles often adhere to surfaces which they strike, but rebounding increases with velocity of impact (Paw 1983).

Other causes of instability include the evaporation of particles, the growth of soluble particles by condensation of vapour, precipitation of electrically charged particles due to induced image charge, and enhanced coagulation by mutual attraction of bipolar charged particles.

Light is scattered and sometimes absorbed by aerosol particles. The combination of these effects results in attenuation or partial extinction of a parallel beam of light as it traverses aerosol, partly by deviation of light away from the original direction and partly by absorption in the particles. The extinction efficiency of a particle is the loss of light travelling in the original direction relative to the amount of light incident upon the particle, that is, the projected area of the particle normal to the direction of illumination multiplied by the intensity of illumination. Particles which are large in size compared with the wavelength of light have an extinction efficiency of 2, independent of the size of the particle and its optical characteristics. When the size is comparable with the wavelength then, if there is not much absorption, the extinction efficiency fluctuates with size because of interference between the illuminating beam and light which has

passed through the particle; the optical properties of the particle are then important. Further decrease in particle size causes the extinction efficiency to decline rapidly (Hodkinson 1966).

Particles which are far from spherical in shape are responsible for some optical phenomena to be seen in the atmosphere; the particles have to be larger than several microns and their scattering power is virtually independent of wavelength since the transmission path is too long for the phase difference causing interference to be appreciable and scattering by diffraction results in only a very slight change of direction. Illumination by white light thus results in white scattered light. Rainbow colours result with much larger droplets and are caused by dispersion of light transmitted through them which, for spheres, gives scattering angles independent of droplet size (Minnaert 1954).

Colours also appear when particles are smaller than about 2 μm and are nearly spherical and uniform in size. First come the higher-order Tyndall spectra, due to interference, and then, below about 0·2 μm diameter, the Rayleigh scattering which is stronger for shorter wavelengths; it is the cause of blue sky and of the red sun seen through a haze of submicron particles (Kerker 1969).

The dynamical behaviour of an aerosol depends on the shapes and sizes of the particles. Rounded, smooth particles of compact shape approximate to the behaviour

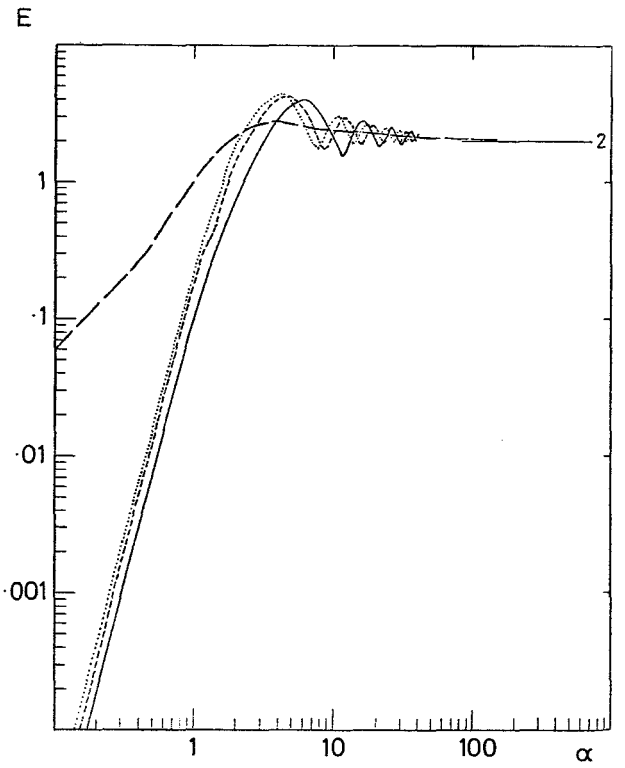

Figure 1. Extinction efficiency, E, of spherical particles as a function of the optical size parameter, $\alpha = 2\pi a/\lambda$. a is the particle radius and λ the wavelength of the light. Transparent spheres: ———, refractive index 1·33; – – – –, refractive index 1·45; ..... refractive index 1·50. Absorbing spheres: — — —, refractive index 1·50–0·3i.

of spheres; their trajectories can be calculated from the aerodynamic drag force, according to Stokes's law, and the inertial force which arises when a particle changes its velocity. Dynamical problems are conveniently generalized by employment of the 'aerodynamic diameter' of particles. This was first defined as the diameter of a sphere of unit density which has the same falling velocity as the particle. It is equal to the diameter of a spherical particle multiplied by the square root of its density and is useful for describing the aerodynamic behaviour of particles (Griffiths *et al.* 1984).

In many situations the particles of an aerosol are sufficiently far apart to act independently. This is not the case in aerosols of high concentration by number of particles. Optical effects are then modified by the light which has been scattered by one particle being scattered again and again by other particles, so that some of it is returned to the direction of the original beam and the original angular distribution of light scattered by the first particle is blurred. This is known as multiple scattering. The aerodynamic behaviour of individual particles at low concentration is not subject to mutual interference with other particles; as a result, all the particles settle under gravity at the appropriate velocities. In concentrated aerosols there is strong mutual action and the aerosol cloud settles as a whole at a faster velocity (Fuchs 1964, p. 46).

Many calculations of the motion of a particle under gravity or in a flowing aerosol are made by approximating it as a sphere or by using the aerodynamic diameter (with unit density) and taking an average orientation if it is far from spherical. Stokes's law of the drag of spheres in viscous flow (equation (20)) is valid within 10% if the Reynolds number, vd/ν, of the sphere moving through the gas is below 0·82. The Reynolds number of a moving object is the ratio of the inertial force which acts upon it, due to its acceleration of nearby fluid, to the viscous drag of fluid upon it. v is the velocity of the particle, d its diameter and ν the kinematic viscosity of the fluid.

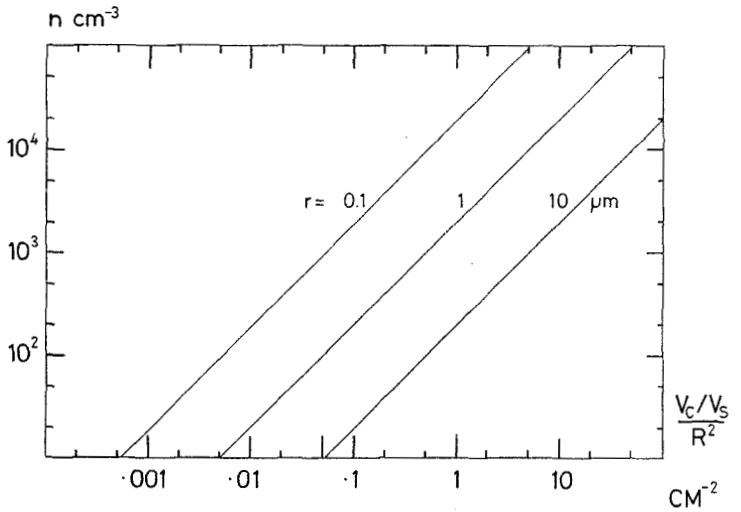

Figure 2. Settlement of a cloud of aerosol particles. Individually the particles fall according to Stokes's law with velocity v_s (equation (24)). A cloud of radius R may fall more quickly if it entrains air and tends to fall as a whole with velocity v_c. The ratio $(v_c/v_s)/R^2$ can be read off this diagram for particles of radii 0·1, 1 and 10 μm and concentrations from 10 to 10 000 cm^{-3} (Fuchs 1964, p. 48). Circumstances may cause the air entrained in the cloud to have a different density from the air outside, in which case this diagram should not be used.

When the Knudsen number of a spherical particle (mean free path of the gas molecules/radius of particle) is equal to 0·08 the drag is 10% less than the Stokes's law value and decreases further for smaller spheres, that is higher values of the Knudsen number. Hence, for particles smaller than 1·7 μm diameter in ordinary air it is necessary to apply the Cunningham–Knudsen–Weber–Millikan factor (equation (31)) to the Stokes's law drag (Egilmez and Davies 1982). The reason is that when the size of the particle is comparable with, or less than, the mean free path of the gas molecules the particle tends to unimpeded motion, as in a vacuum.

Several methods of describing the morphology of aerosol particles have been proposed. Extreme shapes result in complicated dynamical behaviour depending on the orientation of the particle. Replacement of a particle by a dynamically equivalent spheroid is of limited value because real particles may have sharp edges and surface complexities which considerably affect the Stokes's law, viscous flow drag. The subject has been discussed by the writer (Davies 1979 a).

Because of the strong dependence of the behaviour of aerosol particles upon their size, it is not easy to interpret the results of experiments with aerosols of particles covering a wide range of sizes. This problem has been dealt with in two ways. Inhomogeneous aerosols are often sampled with size-selecting devices which separate the catch into two or more fractions of less inhomogeneous particles. Alternatively, experimental work is often carried out with aerosols in which the range of sizes present has been limited by a special method of generation aimed at the production of near-homogeneous aerosols. Such aerosols can occur in nature. The instability of an aerosol containing a wide range of particle size causes it to become more homogeneous as it ages.

2. Measuring the aerosols of the atmosphere

Leonardo da Vinci (1452–1519) believed that the blue colour of the sky was due to the illumination by sunlight of small particles of moisture in the atmosphere. Measurements of the number of atmospheric particles were first made by Aitken in 1888; he constructed 'dust' counters in which a sample of air was moistened and then cooled by expansion so that the particles acted as condensation nuclei and condensed water vapour until they were large enought to be seen and counted, after settlement. The least size of the original particles which would grow depended on the expansion ratio, the critical size for insoluble particles being larger than for soluble ones since soluble material in the particles dissolves in and lowers the equilibrium vapour pressure of condensed water, causing growth to commence at a lower relative humidity than when pure water exists on the surface of insoluble particles. The first to show the part played by particles in the condensation of water vapour in air was Coulier, in 1875, but he was unable to explain his experiments and the work came to nothing. It is discussed by Aitken in his collected papers, p. 65.

Aitken (1923) demonstrated with his instruments that atmospheric nuclei were generated by flames and dispersed into the atmosphere. He also found that they were given off by platinum and other metals and solids when red hot. Electrical discharges in air were shown to create particles. He experimented on gas-to-particle conversion, showing that exposure to sunlight of air containing SO_2, in a glass flask, failed to produce the nuclei which resulted when the gas was exposed in a flask made of silica. The silica flask admitted ultraviolet rays from the sun which caused the SO_2 to oxidize and produce fine sulphate particles. He commented on the enormous amounts of

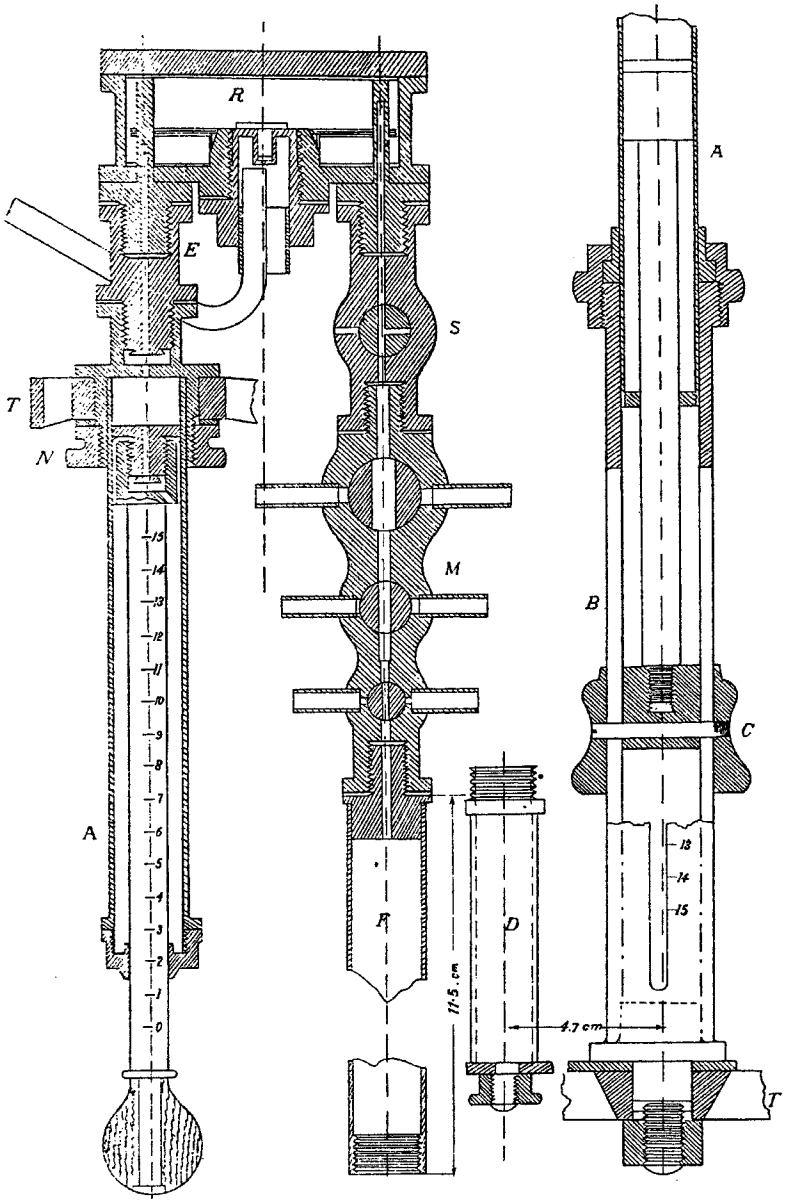

Figure 3. An Aitken nucleus counter (Aitken 1923, p. 283). A sample containing a suitable number of particles is collected in the barrel of one of the stopcocks, M. Diluting, clean air is drawn in by the pump, A, through the filter, F, leaving the chamber, R, filled with a diluted sample. R is lined with moist blotting paper. Stopcock S is then closed and the expansion is made with the pump causing moisture to condense on the nuclei in R which then settle on the stage in R and can be counted with a lens. (Cambridge University Press).

sulphur products which were injected into the atmosphere by burning coal, due to its content of sulphur. He found the air to be greatly polluted with nuclei produced by human activities and demonstrated the existence of masses of clean air and of polluted air which travelled many miles.

The temperature, T_2, produced by adiabatic expansion of a perfect gas from V_1 to V_2, with an initial temperature T_1, is

$$T_2 = T_1(V_1/V_2)^{0.403} \tag{1}$$

and the corresponding ratio of total pressures is

$$P_1/P_2 = (V_2/V_1)^{1.403} \tag{2}$$

where 1·403 is the ratio of the specific heats of dry or moist air. If p_1 is the initial water vapour pressure in the air at T_1 before expansion and p_2 the saturation water vapour pressure after expansion at T_2, the saturation ratio S is given by

$$S = (p_1/p_2)(P_2/P_1) \tag{3}$$

Knowing S, the minimum diameter, $d_{\min}$, of an insoluble particle which will nucleate water drops can be found from the Maxwell–Kelvin equation

$$d_{\min} = 4\gamma M/(\ln S \cdot R_M T_2 \rho) \tag{4}$$

where γ, M and ρ are the surface tension, molecular weight and density of water at T_2 K and R_M is the gas constant per mole.

Using these equations the theoretical performance of condensation nucleus counters (CNC) has been calculated over a range of expansion ratios and the results are shown in table 1 for $T_1 = 293$ K, $P_1 = 760$ torr. In Aitken's instruments the expansion was not adiabatic so the temperature fall was less. The most accurate determinations of the numbers of Aitken nuclei in the atmosphere in many parts of the world are now made with the Nolan–Pollak condensation nucleus counter, the development of which has been outlined by Pollak (1959) and Nolan (1972). The grown droplets partially extinguish a converging light-beam which passes along the axis of the condensation tube. The axial beam is an important feature since the expansion in the central region of the tube is adiabatic (Garland and Branson 1977) and loss of particles by diffusion to the wall of the tube is reduced. A study of the degree of supersaturation obtained has been described by Padma *et al.* (1984), who concluded that a Gardner counter was likely to underestimate considerably particles (presumably insoluble ones) which were smaller than 5 nm in diameter. The Gardner is a portable CNC which is usually calibrated against a Nolan–Pollak.

Calculation of the size of the smallest nucleus which condenses water according to equation (4) has been questioned on the grounds of a diminution of the surface tension of liquid in very small droplets, analogous to the rise in vapour pressure; this is fallacious. The equilibrium vapour pressure is greater for small droplets than the value for a flat surface of water because the attraction of an escaping vapour molecule by molecules in the liquid is less, due to the sharp curvature of the surface; the molecular attraction, in this case, operates over distances of several molecular diameters. Surface tension is due to the mutual attraction of molecules in contact and is therefore not

Table 1. Minimum diameters, d_{min}, of insoluble spheres which will nucleate water droplets, in air saturated with water vapour at 20°C and 760 torr, on adiabatic expansion.

Expansion ratio, V_2/V_1	Pressure ratio, P_2/P_1	Temperature drop $(T_1 - T_2)$ degrees	Sat.w.v.p. at T_2: p_2 torr	Saturation ratio, S	d_{min} (μm, nm)	Nature of particles
1·00002	1·000028	0·00236	17·530	1·00026	8·2 μm	
1·00005	1·000070	0·0059	17·527	1·00040	5·3 μm	
1·0001	1·000140	0·0118	17·520	1·00070	3·0 μm	
1·0002	1·000280	0·0236	17·507	1·0013	1·64 μm	Nuclei of haze
1·0005	1·00070	0·0590	17·470	1·0030	0·71 μm	and mist
1·001	1·00140	0·118	17·407	1·0059	0·36 μm	
1·002	1·0028	0·236	17·281	1·0119	0·18 μm	
1·005	1·0070	0·588	16·91	1·030	72 nm	
1·01	1·014	1·173	16·30	1·061	36 nm	
1·015	1·021	1·748	15·72	1·092	24 nm	Non-nucleating
1·02	1·028	2·328	15·16	1·125	18 nm	atmospheric
1·03	1·042	3·470	14·10	1·193	12 nm	particles; range
1·05	1·071	5·75	12·18	1·345	7·2 nm	of condensation
1·10	1·143	11·0	8·61	1·782	3·7 nm	nucleus counters
1·146	1·211	15·7	6·23	2·324	2·5 nm	
1·20	1·292	20·7	4·35	3·12	1·86 nm	
1·26	1·383	26·1	2·91	4·36	1·45 nm	Negative ions
1·30	1·445	29·5	2·24	5·66	1·23 nm	Positive ions
1·33	1·492	31·8	1·86	6·32	1·16 nm	Large molecules
1·38	1·571	35·7	1·16	9·62	0·94 nm	Large molecules

affected by the size of liquid droplets containing many molecules. There are over 400 water molecules in a droplet of 1·5 nm radius.

The standard type of Nolan–Pollak condensation nucleus counter (CNC) is the 1957 model with convergent light-beam. It is filled with aerosol and pumped to an excess pressure of 160 torr, making P_1/P_2 equal to 1·211. On expanding back to

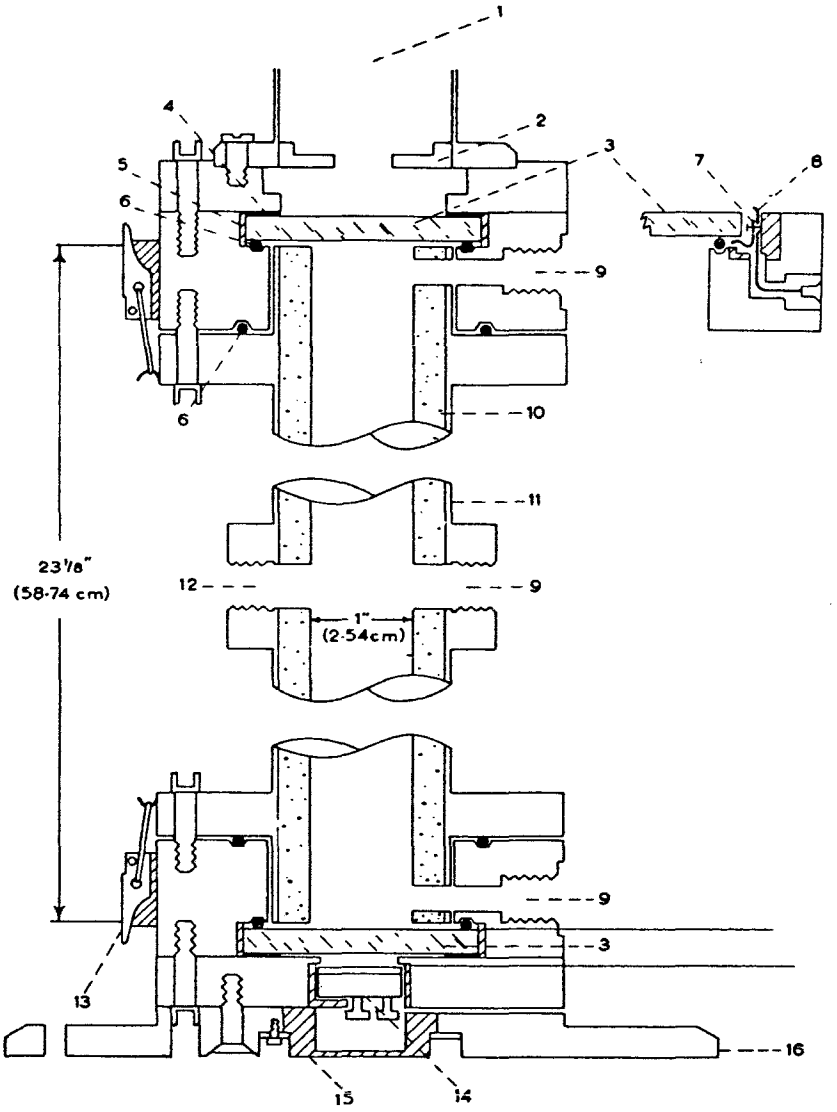

Figure 4. A Nolan–Pollak condensation nucleus counter, 1, Lamp house; 2, stop 9/16″; 3, electrically heated glass sealing plates; 4, rubber compression ring; 5, insulator; 6, O-ring; 7, spring contact for electrical contact to conducting glass sealing plate; 8, connecting wire and terminal for electrical current heating sealing glass; 9, threaded connections for vacuum taps; 10, removable porous ceramic lining, external diameter 4 cm, diameter of central bore 2·5 cm; 11, fog-tube, internal diameter 4 cm; 12, threaded port for insertion of test probes (e.g. resistance thermometer); 13, quick action toggle clips; 14, photo-electric selenium cell; 15, housing for photocell; 16, base plate. (School of Cosmic Physics, Dublin).

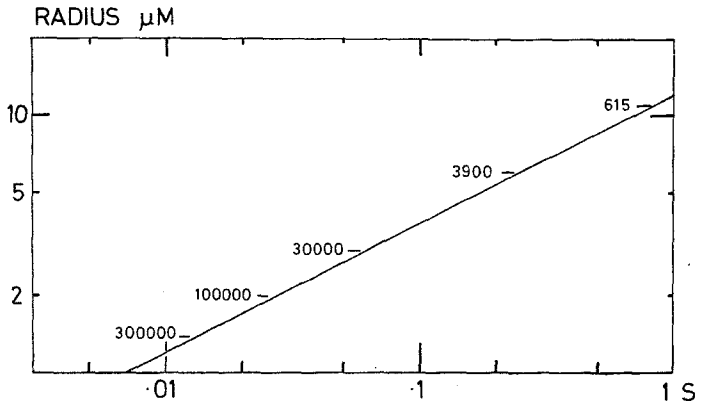

Figure 5. Growth of droplets in the Nolan–Pollak counter. Growth ceases when all the available water is used up, hence low concentrations of nuclei result in large droplets; this is the reason why calibration is necessary; the approximate concentrations of droplets per cm^3 are marked on the line.

760 torr, table 1 shows that a saturation ratio of 2·324 is achieved, which should make insoluble particles 2·5 nm diameter and larger grow by condensing water vapour. In fact, over 70% of the particles of this size are lost in the instrument by diffusion during the 'dwell time' before the expansion (Egilmez and Davies 1984); the loss becomes negligible for particles larger than about double this size. The final calibration for this instrument was given by Pollak and Metnieks (1960) and differs slightly from previous ones (Bodhaine and Murphy 1980, Hogan and Barnard 1983).

It has been claimed by Sinclair (1984) that the Nolan–Pollak instrument undercounts nuclei when the concentration exceeds $10^5/cm^3$, which is questioned by Davies and Egilmez (1985). The issue is discussed by Davies and Egilmez (1986) and Sinclair and Knutson (1986), from which it seems that the latter believe the temperature of air expanded adiabatically to be higher if the air is moist; this is wrong because the drop for perfect gases is independent of the molecular weight except for the ratio, 1·403 which does not change appreciably with the moisture content of the air. The size to which droplets grow is limited by the amount of water available and depends on the concentration of nuclei; under standard operating conditions it is 1·1 μm for $6{\cdot}4 \times 10^5$ particles/cm^3 and 11·2 μm for 615/cm^3 (Davies and Egilmez 1985). This variable size makes calibration necessary over the range of concentrations.

The size to which the nuclei grow does not depend appreciably upon the initial size of the nuclei, but if the nuclei are soluble in water the values of d_{min} (equation (4)) will be much less than those given for insoluble particles in table 1. Hence the presence of even very small, soluble Aitken nuclei increases the count; fewer soluble particles are lost by diffusion since they grow at 100% RH during the dwell time.

The data shown in table 1 are divided into three groups. The first seven lines relate to saturation ratios which are encountered in the atmosphere, where values exceeding 1·01 (101% RH) are extremely rare; hence, insoluble nuclei smaller than about 0·2 μm diameter cannot nucleate atmospheric water droplets. However, soluble nuclei which are much smaller than this are able to do so, down to sizes depending on the solubility. This is illustrated for sodium chloride particles in table 2 which is based upon the calculations of Zebel (1956); for a diameter of 0·2 μm the size of the droplet which such a

Table 2. Growth of sodium chloride particles in the atmosphere.

nitial diameter (μm) of solid particle for R.H. < 76·3%	Diameters (μm) of liquified particles at percentage relative humidities					
	85	95	98	99	100	101
0·01	0·01	0·0214	0·0230	0·0236	0·0244	0·0260
0·02	0·04	0·048	0·056	0·062	0·076	0·088
0·1	0·21	0·27	0·37	0·46	0·75	0·80
0·2	0·42	0·56	0·76	0·96	2·22	unlimited growth
1·0	2·2	2·8	3·9	5·0	24	unlimited growth
2·0	4·2	5·8	8·0	10·4	68	unlimited growth
10	22	28	38	50	780	unlimited growth
20	42	58	80	104	2200	unlimited growth

particle nucleates is over five times larger at 100% RH and will grow indefinitely in the atmosphere at the limit of 101%. Growth is only small for a sodium chloride particle which is initially 0·01 μm in diameter and can produce a drop of 0·026 μm at 101% RH. The larger the soluble particle, the greater is the number of times the nucleated drop will grow to in the atmosphere. The growth with increasing relative humidity of droplets after nucleation by other soluble compounds has been discussed by Orr *et al.* (1958), Winkler (1973), and Tang (1976).

Insoluble nuclei in the atmosphere which participate in the nucleation of atmospheric water droplets, and are therefore larger than about 0·2 μm diameter, cannot be counted with a Nolan–Pollak condensation nucleus counter or analogous instruments. Of the soluble nuclei, smaller sizes down to about 0·01 μm can be counted but unlike the larger nuclei they do not grow in size indefinitely at high relative humidities, as shown in table 2, so that there is an upper limit to the size of grown droplets created by these nuclei. They are responsible for haze which is perceived over long distances (Davies 1974a, 1975) and increasingly reduces visual range as the humidity rises (figure 6).

A special type of condensation nucleus counter has been designed by Leaitch and Megaw (1982) for use over the range of relative humidity from 100·04% to 100·4%. This counts insoluble particles in the range 5 to 0·5 μm diameter and soluble ones between 0·25 and 0·025 μm diameter, approximately. Most of these are too large for the Nolan–Pollak type of instrument.

The second section of table 1, lines 8 to 16, covers the ranges of expansion and adiabatic cooling which are theoretically possible in the Nolan–Pollak instrument. The figures were calculated independently and agree with those of Miller and Bodhaine (1982). Insoluble particles of the sizes which condense water and grow, run from 2 to 70 μm diameter and do not nucleate water droplets in the atmosphere; soluble particles will be counted with expansions below 1·03 and are able to nucleate droplets in the atmosphere.

The bottom section of table 1, lines 17 to 20, shows that, in the absence of particles, condensation is produced at large expansion ratios on ions and large molecules of vapour, or clusters of molecules.

Condensation nucleus counters of a number of different designs are in use, including absolute instruments of high accuracy (Schmitt *et al.* 1982) and more portable instruments, intended to be easier to operate, which are often inferior in performance

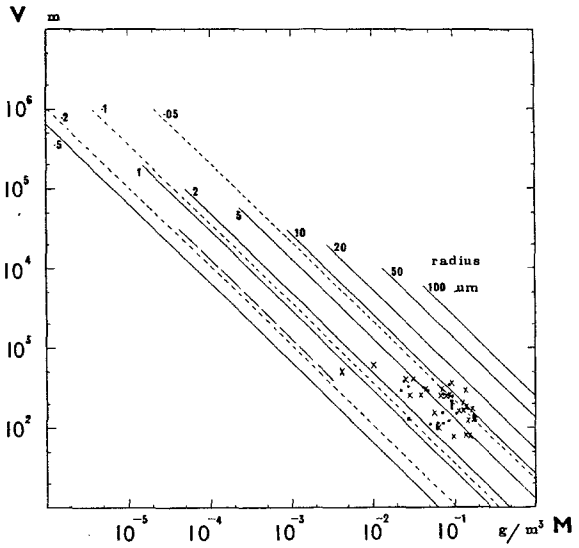

Figure 6. Visual range, Vm, through homogeneous mists of water droplets against mass concentration, M g/m^3, for particle radii 0·05 to 100 μm. The experimental points are from observations in mist (×, ·) and smog (——).

(Roddy and O'Connor 1981). The 1957 standard Nolan–Pollak instrument has played an important part in determining the concentration of the smaller atmospheric particles in many parts of the world, both directly and as a reference standard. A fortyfold range of diameters is covered, say 0·003 to 0·1 μm, and the counts are not very dependent on the humidity of the atmosphere. Few of the particles counted are involved with the formation of atmospheric water droplets so it is better to call them Aitken nuclei rather than condensation nuclei since the latter function is not performed in the atmosphere but only in the measuring instrument, with its high saturation ratio of 2·32.

Accurate calibration at other saturation ratios (Nolan and Pollak 1946) has not been carried out, so using the instrument to determine size distribution, as described by Egilmez and Davies (1982), is not common. The aerosol which is admitted to the CNC can be passed through a diffusion 'denuder' which removes small particles so that a size distribution can be obtained by making repeated measurements at the standard compression with different adjustments of the denuder (Flyger *et al.* 1976). Size distributions of ions can be obtained by passing the aerosol between charged parallel plates, which removes ions; they carry unit charges, on account of their small size (Megaw and Wells 1971). Since the air-drag of a larger ion exceeds that of a smaller one, the latter has higher mobility and is deposited first and thus the size can be calculated from the mobility. More recently the aerosol particles have been charged artificially, graded according to mobility and the respective numbers taken to be proportional to measured ion counts. Difficulties, mainly associated with charging, have been encountered with such apparatus, especially for small particles (Bricard *et al.* 1981). The design and use of diffusion batteries for analysis of the size distribution of aerosols with particles below 30 nm diameter has been described by Brown *et al.* (1984) and Scheibel and Porstendorfer (1984).

Atmospheric particles which are too large for the Nolan–Pollak instrument have been sampled from balloons and aircraft up to altitudes of 30–40 km using impactors or photoelectronic counters of single particles (Junge and Manson 1961, Bigg *et al.* 1971, Bigg 1976, Gras 1978). Particles having diameters above about 0·1 μm can be recorded.

In order to estimate the total number of particles in a vertical cylinder of the atmosphere from a limited number of observations made at different heights it is useful to have an interpolation formula expressing the size distribution of all the particles in the vertical cylinder. The form used by Shaw (1976) is

$$\frac{dN}{dr} = ar^2 \exp(-2r/r_m)\,\mathrm{cm}^{-3} \tag{5}$$

where N is the total number of particles in a vertical cylinder of 1 cm^2 cross-section extending from the surface of the earth to the top of the atmosphere ($\sim$40 km). The concentration of particles becomes extremely small at such altitudes so that the actual height does not need to be accurately defined; r is the particle radius which is equal to r_m at the peak value of dN/dr. The units of a are cm^{-5}.

Integration of equation (5) shows that the total number of particles in the vertical cylinder is

$$N = \tfrac{1}{4} a r_m^3\,\mathrm{cm}^{-2}. \tag{6}$$

The total volume of all the particles is Vcm^3/cm^2,

$$V = \frac{4\pi}{3}\int_0^\infty r^3 \frac{dN}{dr}\,dr = 2{\cdot}5\pi a r_m^6 = 10N\pi r_m^3\,\mathrm{cm} \tag{7}$$

and the total weight,

$$M = \rho V\,\mathrm{g/cm}^2. \tag{8}$$

From observations at the South Pole, Mauna Loa and Alaska, Shaw (1976) gives values of r_m of 4×10^{-6} and 9×10^{-6} cm, N from 48×10^6 to 114×10^6 cm^{-2}, and of ρV, where ρ is the density of the particles, from $2{\cdot}3\times10^{-7}$ to $9{\cdot}6\times10^{-7}$ g cm^{-2}. These figures indicate that a varies from 10^{23} to 7×10^{24} cm^{-5}.

If I_0 is the intensity of sunlight outside the atmosphere and I is the intensity on the ground, and it is assumed that the atmospheric particles act independently without appreciable secondary scattering,

$$(\cos\zeta)\ln\frac{I}{I_0} = -2\pi\int_0^\infty N_r E_r r\,dr = -O \tag{9}$$

where ζ is the zenith distance of the sun, N_r the number of particles of radius r in the vertical cylinder of atmosphere, and E_r their extinction efficiency which depends on their refractive index and absorption coefficient.

O is a dimensionless number which is known as the vertical optical depth of the atmosphere; it is sometimes referred to as the dust index, the opacity or the turbidity. In the absence of gas molecules and particles O would be equal to zero; the more the sun's light becomes obscured, the greater is O. For example, when $O=4$ the transmission, I/I_0, of sunlight through the atmosphere is only 1·8%.

By measuring I at different zenith angles with a sun photometer (Flowers *et al.* 1969), I_0 can be estimated from equation (9) (Dyer 1974), and O can be calculated. If the sizes and composition of the atmospheric particles are known, E is defined over the size

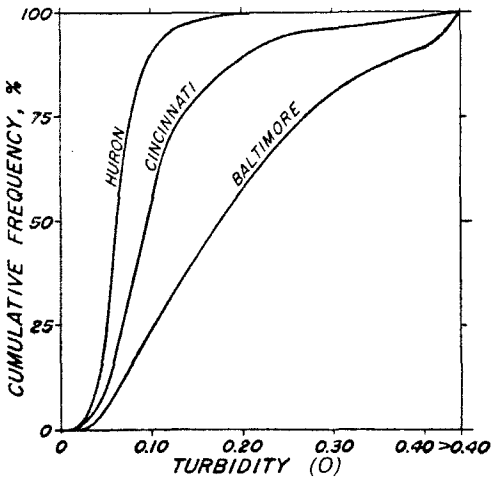

Figure 7. Cumulative frequencies of occurrence of daily average atmospheric turbidity for rural (Huron), suburban (Cincinnati) and urban (Baltimore) districts. (Flowers *et al.* 1969). (*J. appl. Meteorol.*).

range and O can be calculated independently. The importance of monitoring the value of O is that an increase with time might be an indication of an increasing extent of the pollution of the atmosphere due to human activities, over and above the various natural sources of atmospheric particles. The global climate is sensitive to the value of O.

Volcanoes have produced readily detectable, sudden increases in the value of O, which are greatest when observed from the same latitude as that of the eruption. The increased optical depth may persist for several years, with seasonal variation, due to dust having penetrated to the stratosphere; values of O are mostly below 0·01 ($I/I_0 = 0{\cdot}99$) except near the volcano. During the first week of the Mount St. Helens eruption (Merchant *et al.* 1982) airborne dust concentrations in Yakima, the nearest city, averaged 13·3 mg/m^3 and fallout was up to 10 cm thick over a large area.

Dyer (1974) made an analysis of values of O over a period of 90 years which embraced a number of major volcanic eruptions. He finally concluded with the definite impression that no significant change in atmospheric turbidity had taken place during the period 1916 to 1959. Estimates of aerosol emissions by Benarie (1981) are relevant to this conclusion. A large volcanic eruption might put 10^{14} g of dust into the atmosphere with a decay time exceeding 10 days. The annual blow-off from deserts was reckoned to contribute five times more than the single volcanic eruption. However, the annual emission due to man's activities was only about a third of the latter.

A summary of global particulate emissions was prepared by Robinson and Robbins (1971). The total was $2{\cdot}6 \times 10^9$ tons/year of which 88·5% had natural origins and 11·5% was pollutant due to human activities.

Such estimates at the above are very approximate. The global airborne particulate yield from forest fires is given by Robinson and Robbins (1971) as 3×10^{12} g/year whereas the figure for the USA alone is given by Sandberg *et al.* (1979, figure 3) as $3{\cdot}2 \times 10^{12}$ g/year, which would suggest a global figure some 10 times larger. Smith (1981, table 3–16) gives only 0·5 to 0·7 $\times 10^{12}$ g/year from 1970 to 1976 for forest fires in

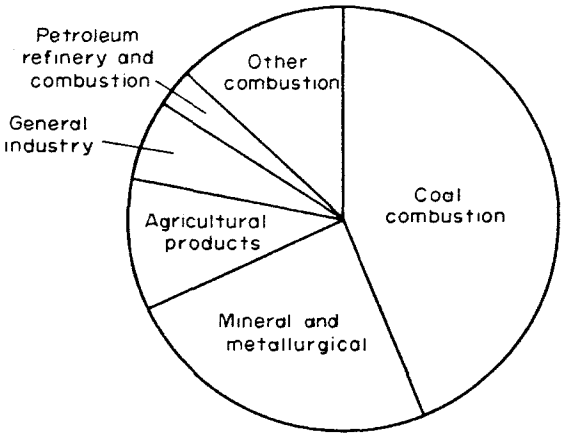

Figure 8. Relative masses of man-made emissions of particles into the atmosphere (Robinson and Robbins 1971). (Stanford Research Institute.)

the USA. Figures for the ratio of mass of airborne particulate to mass of fuel vary between 0·003 and 0·15.

A possible cause of climatic change is the aerosol projected into the atmosphere by the impact of large meteorites or by ground or near-ground nuclear explosions. Some data are given in table 3. The optical depths, O, have been calculated on the basis of 3×10^5 g of dust being dispersed into the atmosphere per megaton (Turco *et al.* 1983) and normalized on the basis of the mass per unit area in a vertical cylinder of atmosphere being constant over half of the earth's surface ($2{\cdot}5 \times 10^{18}$ cm^2). The orders of magnitude of the optical depths have been obtained by integrating equation (9) with N_r constant and $E_r = 1$, giving

$$O \simeq \pi N r_m^2 \tag{10}$$

From (7) and (8)

$$M = \rho \times 10 N \pi r_m^3 \tag{11}$$

and using (10) to eliminate N,

$$O = M/10\rho r_m \tag{12}$$

r_m has been taken as 6×10^{-6} cm, following Shaw (1976) and ρ as 2·5 g/cm^3, giving

$$O \simeq M/1{\cdot}5 \times 10^{-4} \tag{13}$$

For $r_m = 2{\cdot}5 \times 10^{-5}$ (Turco *et al.* 1983), O would be four times larger than the values of table 3.

The values of O in table 3 do not suggest that any substantial change of climate can result from the dust dispersed into the atmosphere other than by the impact of a very large asteroid ($2{\cdot}7 \times 10^{-10}$ of the mass of the earth), or by the explosion of a 10^{14}-ton nuclear device. However, it is argued that the focal release of a very large amount of energy would cause a huge firestorm and that the dense smoke cloud formed, 32 km in diameter from a 1-Mton nuclear explosion, would be more effective in creating a nuclear winter than the dust dispersed by the blast.

Table 3. Dust loading of the atmosphere above a hemisphere of the earth following a large energy release.

Agent	Age (M years)	Mass (g)	Crater diam. (m)	Energy (Mton)	Dust load, M (g/cm^2)	O	References
Holleford meteorite	700	$3{\cdot}6 \times 10^{14}$	2349	14	$1{\cdot}7 \times 10^{-12}$	$1{\cdot}1 \times 10^{-8}$	Innes (1961)†
Brent meteorite	700	$1{\cdot}1 \times 10^{15}$	3505	46	$5{\cdot}5 \times 10^{-12}$	$3{\cdot}7 \times 10^{-8}$	Innes (1961)†
Deep Bay meteorite	70	$4{\cdot}9 \times 10^{16}$	12192	1900	$2{\cdot}3 \times 10^{-10}$	$1{\cdot}5 \times 10^{-6}$	Innes (1961)†
Asteroid or comet Italy, Denmark and New Zealand (iridium excess)	65	$1{\cdot}6 \times 10^{18}$	>100,000	$7{\cdot}10^{7}$	$8{\cdot}4 \times 10^{-6}$	0·06	Alvarez *et al.* (1980)‡ Pollack *et al.* (1982)§
Nuclear explosion	—	—	—	1	$1{\cdot}2 \times 10^{-13}$	8×10^{-10}	

† Innes, M. J. S., 1961, *J. geophys. Res.*, **66,** 2225–2237.
‡ Alvarez, L. W., *et al.*, 1980, *Science, N. Y.*, **208,** 1095–1169.
§ Pollack, J. B., *et al.*, 1983, *Science, N. Y.*, **219,** 287–289.

The value of O in table 3 for the huge asteroid corresponds to a 6% loss of solar intensity. Four times the value, 0·24, is a 21% loss. This could have a global effect on its own. Hence, if the extinction of earlier forms of life on earth was due to such a catastrophe, the size of the colliding asteroid must have been enormous.

3. Generation of aerosols in the atmosphere

Aerosols originate in two basic ways: the fragmentation of the raw material, either solid or liquid, followed by dispersion of the particles, or the condensation of vapour molecules as a result of a gas-phase reaction or of supersaturation produced by supercooling.

Dusts formed from solids contain particles over a wide range of sizes, say 0·1 to 100 μm, of shapes reflecting the structure of the parent material. Such aerosols are common in industry, mining, quarrying and tunnelling; if inhaled, they may be a threat to health, particularly if they contain free silica, asbestos, toxic or α-emitting (radioactive) substances. Such industrial dusts are usually quite insoluble in the lungs. Some are hazardous only if they penetrate deeply into the lungs when inhaled and deposit in the alveolated region, consisting of the air cells where gas exchange takes place. Only the finer particles, say below about 5 μm aerodynamic diameter, can penetrate so deeply; larger ones deposit in the airways which are provided with a cleansing system so that the particles, if insoluble, are harmless. Asbestos is exceptional; its longer fibres can penetrate the walls of the airways and produce damage regardless of the site of deposition.

Liquids dispersed by sprays tend to be rather more coarsely sized than dusts but frequently contain soluble poisons and are therefore dangerous to inhale since deposition takes place all along the respiratory tract and droplets which deposit are rapidly absorbed.

Deserts are considerable sources of dust. Darwin, voyaging in the *Beagle*, like many earlier seamen experienced heavy dust falls in the Atlantic which he attributed to the West African Harmattan storms. A considerable amount of research has been directed to the pick-up, transport and ultimate deposition of Saharan dust (Morales 1979); recent studies in Italy have concentrated upon the effect of the dust load upon the opacity of the atmosphere (Prodi and Tomasi 1983, Tomasi *et al.* 1983). By calculating the opacities which would result from postulated dust loads in assumed size distributions and checking with dust samples from raindrops, it was established that mass loadings (equations (7) and (8)) up to 0·5 g/m^2 were possible. The particles were mostly composed of quartz or clay between 0·02 and 2 μm diameter. The design of a new sun photometer and its use to study dust transport across the Sahara has been described by D'Almeida and Jaenicke (1984).

Impactor sampling in Japan, coupled with mineralogical analysis, revealed a two-day influx of yellow sand particles from Chinese deserts 3000 km distant. The mass concentration was 182 μg/m^3 and the size distribution by mass peaked at 4 μm diameter (Ishizaka and Ono 1982).

Combusion processes are responsible for most man-made atmospheric pollution, an important part of which is aerosol. The combustion of coal and oil produces particles from the ash of the mineral content of the fuel. Some 1% of the mass of aerosol is in submicron particles resulting from the condensation of organic vapours of high molecular weight; pyrolysis transforms them into soot. Black aerosol particles absorb heat and light and may have climatological significance for this reason (Hogan *et al.* 1984). Moderate heat produces large spheres and cenospheres (spheres of ash). Very

high temperatures volatilize mineral which condenses to very fine particles, owing to the low vapour concentrations, even at high temperatures, of such involatile substances (Flagan and Friedlander 1978).

The fossil fuels contain sulphur, in varying amounts up to some 3%, which leaves the furnaces as sulphur dioxide; some of this is oxidized to sulphur trioxide, both gases leaving the tall chimneys of, for example, power stations. Sulphuric acid is formed in the atmosphere some of which appears as an aerosol, mainly in fine particles below 0·2 μm. They may contain up to 50% of the total acid emitted. Sulphuric acid has a very low vapour pressure which makes it significant whereas nitric acid is not, on account of its high volatility, unless fixed as nitrate.

It has been estimated that six million tons of sulphur dioxide is exported yearly as gas and aerosol by Britain. There has been concern in Scandinavia about acidification of lakes as a result. A very comprehensive study of Lake Gårdsjön, in south-west Sweden, has been running for some 15 years; the results are now collected into a single volume (Andersson and Olsson 1985). It is concluded that atmospheric deposition contributed 40 to 55% of the total proton input to the soil of the catchment area and that the acidification of the lake was due to direct deposition on the surface of the lake plus an inward flux of protons from the drainage area.

Estimates of global man-made and natural sulphur emissions have been made by Möller (1984).

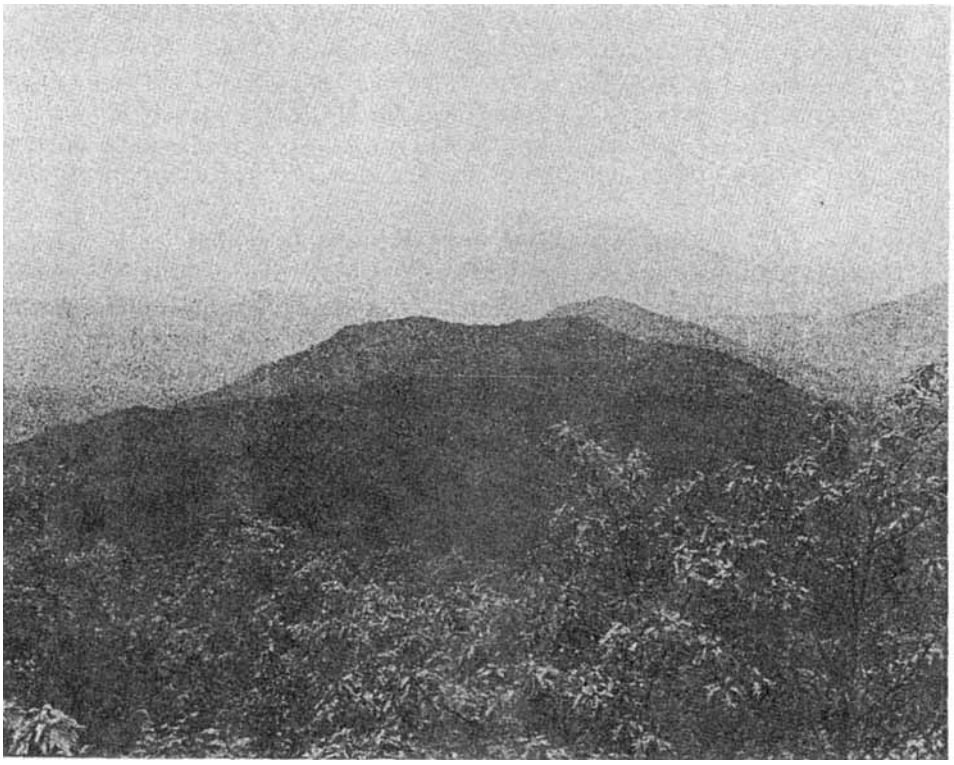

Figure 9. Haze over the Great Smoky Mountains, Tennessee. The particles are below 0·2 μm diameter and are formed by polymerization of terpene vapour emitted by trees. The visibility is about 50 km which corresponds to a particle concentration of 100 $\mu g/m^3$.

A natural contribution to the atmospheric aerosol, with a notable reduction in visual range, is found over forested areas due to the emission of terpenes by trees. Under the right conditions these vapours polymerize to particles under 0·2 μm diameter in concentration up to 100 $\mu g/m^3$ (Davies 1974 a). There is some similarity between this gas-to-particle conversion, aided by sunlight and nitrogen oxide, and the photochemical production of smog from olefins, emitted by internal combustion engines, which convert to peroxyacetyl nitrate and other PAN compounds (Haagen-smit 1952).

Aitken nuclei, particles with diameters below 0·1 μm, are nearly all generated on land. Their origins are combustion (industrial, forest fires, volcanoes) and gas-to-particle conversion of sulphur dioxide and organic gases. None come from the sea.

The oceans were stated by Junge to be the largest world-wide source of aerosol but the marine aerosol is not yet completely understood. The most recent reviews can be found in Roddy and O'Connor (1981, pp. 468–517).

Most of the sea salt is in particles between 2 and 4 μm radius in concentrations exceeding 6 $\mu g/m^3$, depending on wind velocity. The amount of sea salt in particles below 0·5 μm radius is negligible. There is an excess of sulphate; according to Bonsang *et al.* (1981) this might be due to the oxidation of sulphur dioxide produced by photo-oxidation of organic sulphides emitted by algae when exposed at low tide. Renoux *et al.* (1981) observed considerable production of condensation nuclei during daytime low tides and refer to a similar observation by Aitken (1923, p. 495) who recorded up to 150 000 particles per cm^3 on a sunny day. They believed that these nuclei are not produced by sulphur dioxide.

Studies of aerosols in mid-Pacific (Ito 1981) associated them with the trajectories and origins of the air masses. One air mass, which came from Japan, 1000 to 2000 km distant, carried 1000 to 2000 particles/cm^3 with radii peaking at 0·02 to 0·07 μm. An air mass of mid-latitude marine origin carried only 200 to 300 particles/cm^3 with a main peak at 0·02 μm radius and another at 0·04 μm. North Atlantic aerosols are shown by their composition to originate from the land (Gravenhorst and Müller 1981).

4. Size distributions of the atmospheric aerosol

The sizes of atmospheric particles cover such an enormous range ($\sim 10^5$) that it is impossible to sample the full spectrum in a single operation. In polluted air the smallest sizes may be present in some hundreds of thousands per cm^2 and yet weigh less than the few large particles. Sampling of narrow regions of the spectrum has often been carried out for specific purposes, with disregard of the adjacent size ranges; in addition, instrumental failings have been seriously underestimated.

The first appreciation of the total atmospheric aerosol was due to Junge (1963) resulting from many observations with impactors during the 1950s. He showed that a large part of the spectrum could be represented by the distribution by number, N being the total number of particles per cm^3,

$$dN/d\log r = Cr^{-3} \tag{14}$$

where r is the radius of the particles. It will be seen that this means that the distribution by volume, or weight, is constant over the whole range of sizes. This is not a bad approximation over radii between 0·1 and 10 μm, although there is often a dip in the region of 1 μm radius. However, equation (14) predicts too many small particles and often too few large ones. Its virtue is the demonstration of the extremely steep fall in the numbers of particles from 0·1 to about 5 μm radius which is a notable feature of many atmospheric aerosols.

The deficiencies of the formula reflect the inadequacy of single-stage impactor sampling. A condensation nucleus counter is essential for radii below 0·1 μm. Above 5 μm overlaying of small particles by large decreases the small particle counts. Serious entry losses may be due to the inertia of the particles when sampling at a higher velocity than the wind speed and when the sampling nozzle does not face the wind (Davies and Subari 1982). When the sampling velocity is below wind speed too many particles may be sampled (Jayasekera and Davies 1980). The ratio of the number of particles which actually enter a nozzle to the number calculated from the ambient particle concentration and the volume sampled is called the aspiration coefficient.

In dealing with samples it is essential to recover the large particles which deposit inside the nozzle before reaching the proper site of deposition.

The disadvantages of having only a single impaction stage are avoided in cascade impactors; the original 1945 model (May 1945, 1975, 1982) has a lot to recommend it. The same air flow passes through each of the four impaction stages in series but the velocity, V, increases from 2·2 to 34 m/s due to the decreasing areas of the impaction jets.

The efficiency of impaction is a unique function of the Stokes number, St, as long as the geometries of the jets are similar, that is the ratio of width, w, to length, l, is the same. The flow rate is

$$Q = Vwl$$

and

$$St = \tau V/w = \tau Q/w^2 l \tag{15}$$

τ is the relaxation time of the particle. It derives from the equation of motion of the particle (21) where the drag follows Stokes's law. Owing to its mass, a particle does not

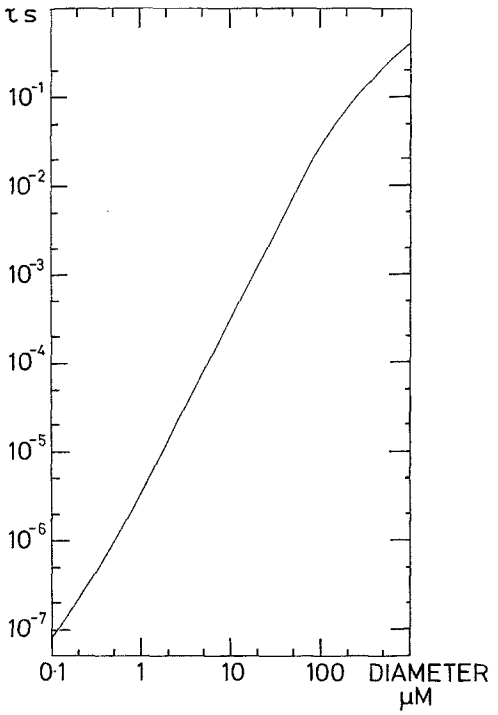

Figure 10. Particle relaxation time, τ, of spheres of unit density in air at 20°C and one atmosphere. τ has been calculated from the sedimentation velocity, $v_s = \tau g$, equation (26) and figure (14).

respond instantly to a change in the ambient air velocity but lags behind a little, while it is 'relaxing' to the new circumstances. It is also the time factor required to reduce the equation of motion (21) to dimensionless form. Hence,

$$\tau F = mF/6\pi a\eta = d^2\rho F/18\eta \tag{16}$$

The Cunningham–Knudsen–Weber–Millikan drag factor, F (equation (31)), is included so that the relaxation times of small particles can be evaluated, since this is required for small, high-speed impactors; d is the diameter of the particles, $(d^2\rho)^{1/2}$ is the aerodynamic diameter, η is the viscosity of air.

The advantage of a cascade impactor is that the separation of coarse and fine particles in four stages avoids the overlapping of a number of fine particles by a single coarse one. The disadvantages are that when the aerosol to be sampled has a high

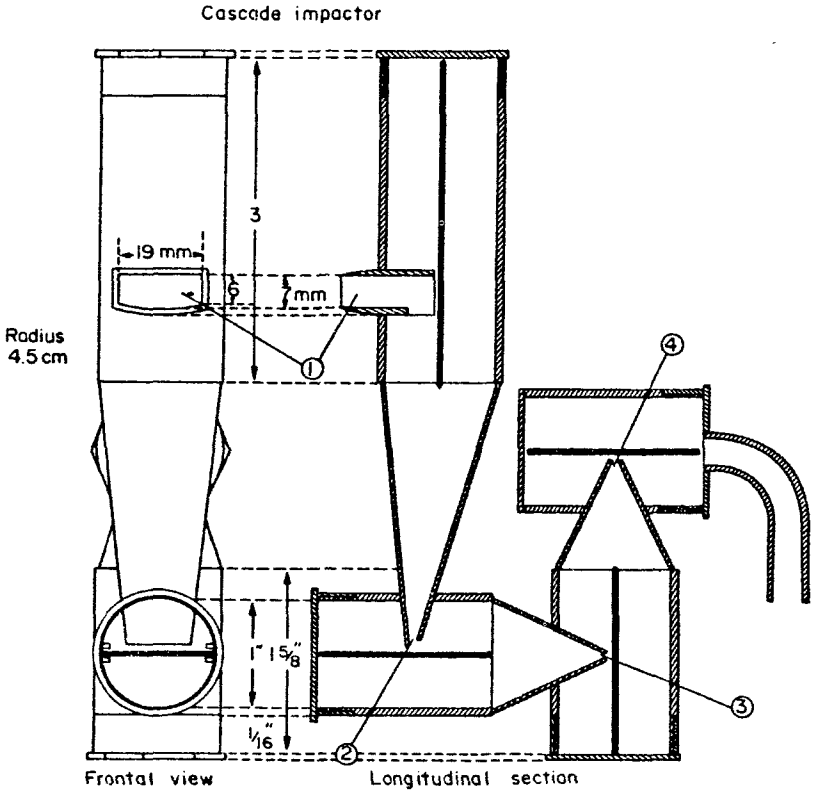

No. of jet	Dimensions of jet (mm)	Clearance between jet and plate (mm)	Velocity through jet at 17.5 l/m (m p h)	Approx. range of particle size of plate (μm)
①	19 x 6.5	5	5	>10
②	14 x 1.6	2	30	20–3
③	14 x 1	1.5	50	y – 1
④	y x 1	1.5	100	3–0.5

(a)

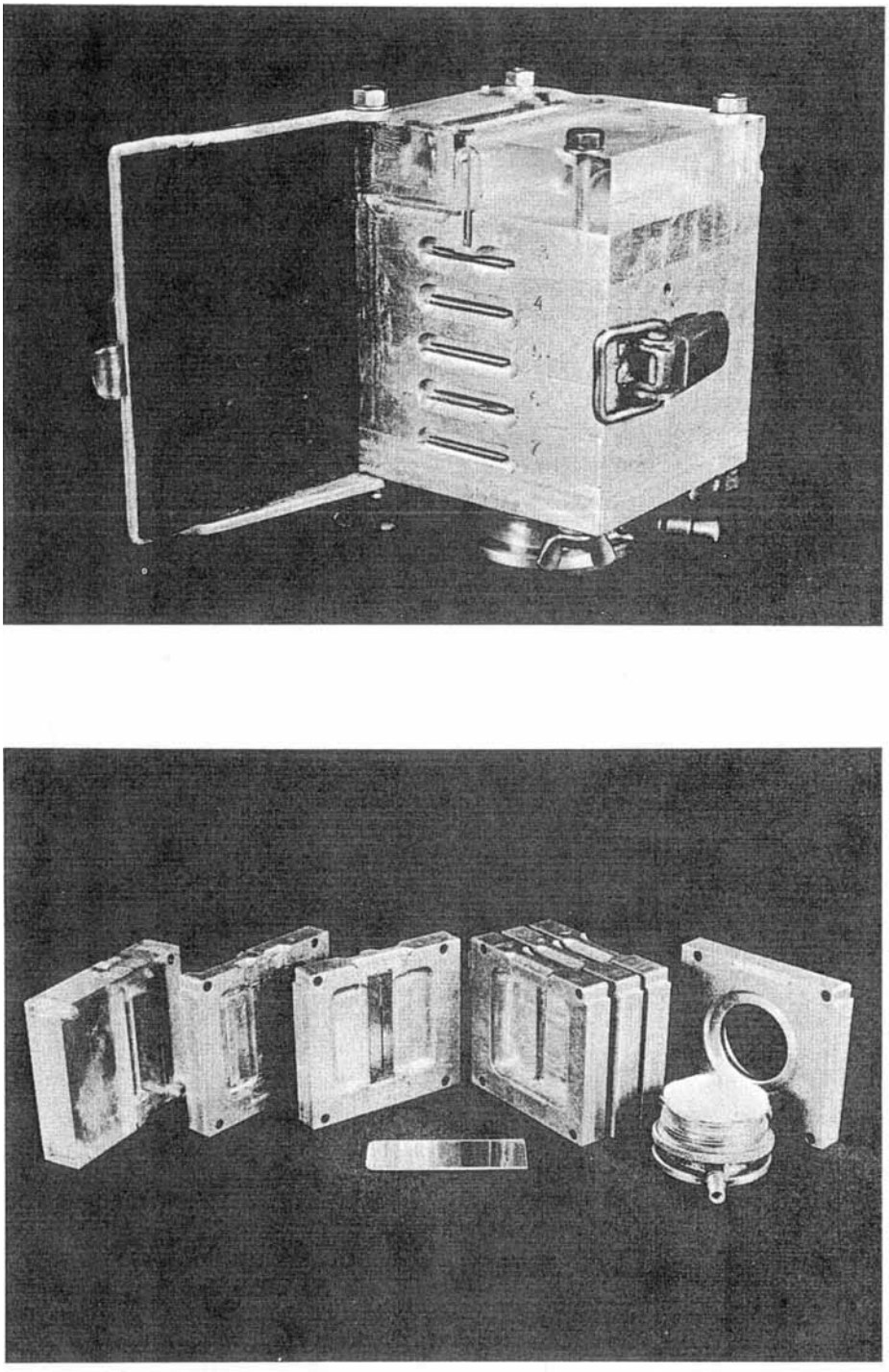

(b)

Figure 11. May Cascade Impactors. (*a*) Standard model (1945) with four stages. Ultimate model (1975) with seven stages of impaction followed by a filter. Designed for minimal internal losses. (*J. Aerosol Sci.* and *J. scient. Instrum.*)

concentration by number of particles, the sampling time may become inconveniently short and there is a tendency for larger particles to bounce after the first impact, which is countered by covering the plates with a film of oil or adhesive (Winkler 1974, Esmen *et al.* 1978).

In virtual impactors the particles are not deposited on plates but their inertial behaviour is employed to divert them into separate air streams from which they can be collected on filters (Masuda *et al.* 1979).

There is a large literature about cascade impactors and many different types have been constructed. Fuchs (1978) has written an 80-page review of the principles and practice of impaction, including a discussion of the main types of cascade impactor. It is remarkable thing that the enormous range of sizes of atmospheric particles can be handled accurately with only two instruments, a Nolan–Pollak CNC, 0·003 μm diameter up to 0·1 μm, and a May cascade impactor from 0·5 to 100 μm diameter, leaving only a small gap between them which is accessible to the recent low-expansion CNCs (Leaitch and Megaw 1982), or, alternatively, to a cascade impactor with a filter backing the last impaction plate or a high-velocity final stage.

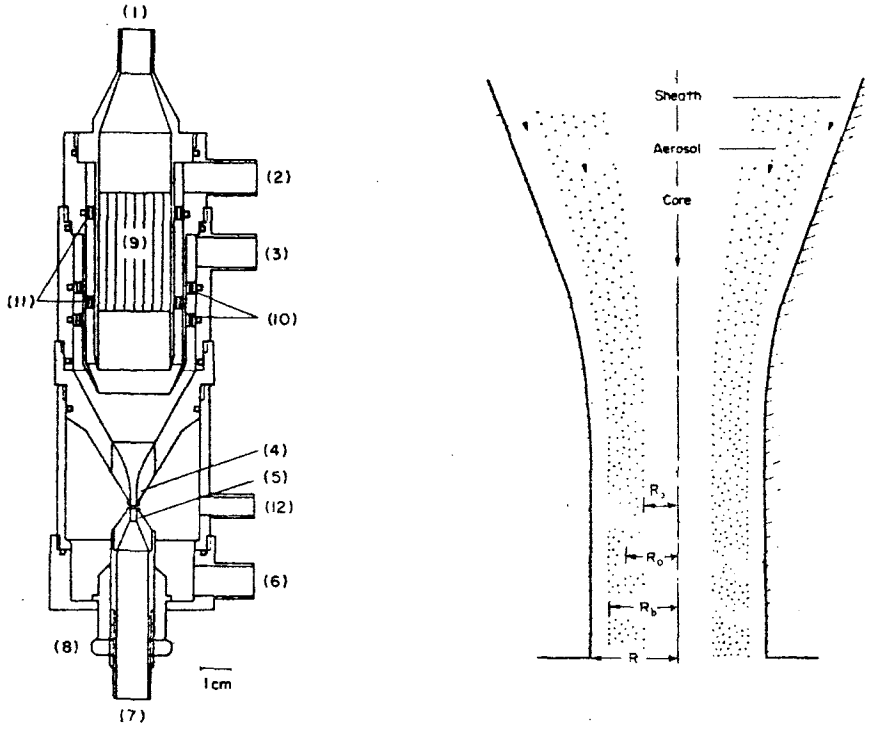

Figure 12. Virtual Impactor (Masuda *et al.* 1979). Aerosol is drawn through the entrance 2 and clean air enters at 1 and 3, creating an annular flow of aerosol between a core and a sheath of clean air. The total flow enters a converging tube and accelerates. Coarse particles, due to their inertia, concentrate in the centre and leave at exit 7. Fine particles are drawn out with the peripheral air by suction at exit 6. Turbulence is discouraged by the honeycomb 9 and by rings of small holes 10, for the aerosol and core flows respectively. (*J. Aerosol Sci.*)

5. Generation of laboratory aerosols

There is a continual demand for generators of relatively monodisperse aerosols in the laboratory for the testing of sampling apparatus and filters. Research on the fundamental properties of aerosols needs such generators.

Laboratory generation of aerosols was reviewed by Kerker (1975) with over 100 references. He divided the methods of generation into condensation (liquid and solid particles), smokes produced by burning, dispersion methods, and other methods (powder dispersal, gas-phase reactions and photolysis). Kerker emphasized techniques of generation which were reproducible and resulted in a narrow size distribution, the so-called homogeneous aerosols.

A drawback of the homogeneous aerosol generators is commonly the low output of aerosol. The spinning-top spray of Walton and Prewett (1949), which is commercially available, is a useful generator. It produces aerosols of quite uniform droplets of liquid from about 15 μm diameter upwards, removing the finer satellite drops (May 1949). Within limits, the size of the final droplets can be reduced by spraying a mixture of volatile and involatile liquids. It can also form aerosols of solid particles by spraying a solution or suspension. The physical mechanisms of this spray were not fully understood. With the aim of revealing them and improving the performance, Davies and Cheah (1984) identified three modes of operation and used dimensional analysis to bring a large number of experimental measurements of sprays and drop sizes into general formulae. Armed with this knowledge, relatively small modifications to the design of the spray were made and losses were reduced; the output of uniform droplets of di-2-ethylhexylsebacate (used because of its low volatility) was increased by a factor of five (Cheah and Davies 1984).

If an ordinary nebulizer is used to disperse liquid the resulting aerosol has a very wide range of particle sizes. Instead of using a spinning disc to produce a near-homogeneous aerosol there is the alternative of selecting droplets over a limited size range from an ordinary spray. This has been done in a very similar way to the inertial selection in a virtual impactor by Suzuki *et al.* (1982). An alternative to the spinning top systems is the vibrating capillary orifice. This idea goes back to 1950; a practical working device is described by Mason *et al.* (1963) and has been improved by Liu (1974). The latter is now commercially available.

Polystyrene spheres of high uniformity can be purchased. Their manufacture is described by Wilkinson *et al.* (1974). Fulwyler *et al.* (1973) describe the manufacture of a variety of spheres, including fluorescent ones. Aerosols can be generated by spraying suspensions of such spheres in a volatile liquid. Some of the problems associated with this method are discussed by Langer and Lieberman (1960), Raabe (1968), Billard *et al.* (1970), Jaenicke (1971) and Fuchs (1973).

Gebhart *et al.* (1980) have written a detailed description of the generation of aerosols from various polymer latices which can be used for producing monodisperse aerosols with particles between 0·05 and 10 μm diameter.

A high-speed rotating disc (6500 rev/s) was built by Tarroni (1971); it would disperse spheres of polystyrene from solution in xylene from 2 down to 0·1 μm diameter and in concentrations up to 10 000/cm^3.

Recent developments in the atomization of liquids are covered exhaustively in some 70 papers presented at the Third International Conference on Liquid Atomization and Spray Systems, ICLASS 85.†

† The proceedings are published by the Institute of Energy, 18 Devonshire Street, London W1N 2AU.

Pressure pack generators of coarse aerosols have considerable commercial importance and are used for a variety of purposes, including medical. The design of the release valve has been fundamental to their success and this has been discussed by Pengilly and Keiner (1977) in connection with the distributions of particle size which are obtainable.

Experimental methods for testing generators, especially with regard to the possible risk of inhaling vapour and particulate effluents by the user, have been described by Mokler *et al.* (1979).

Pressure pack generators can disperse powders in suspension in the liquid filling; a general theory of the distribution of solid particles in the spray droplets has been developed by Callingham (1980).

The design of a breath-actuated medical aerosol inhaler was described by Corr *et al.* (1982); this article was criticised by Newman (1983), followed by a reply from Corr *et al.* 1983.

A variety of methods for the direct dispersal of solid particles has been described, some of which have been reviewed by Hinds (1980), the emphasis being on dust feed systems.

Willeke *et al.* (1974) describe the development of fluidized-bed systems and their application to the dispersal of dusts. They used two-component systems with 100 μm-diameter bronze spheres which gave almost complete deagglomeration and dispersal. Wet and dry beds were used and size distributions are given.

Spurny (1981) describes a vibrating bed generator which works with powders of particles of compact shape or with fibres. The dust is supported on a membrane filter through which air flows while the bed is vibrated with adjustable frequency up to 100 Hz and amplitude up to 1·2 mm. Coarser particles are dispersed at higher amplitudes but the mass concentration peaks at an optimal frequency. Very steady outputs of aerosol can be obtained. The bed can be used with a single-component material or as a two-component bed with glass spheres added for pulverization.

Another double-component system is described by Boucher and Lua (1982) which yields high concentrations of dusts, up to 4 mg/m^3 in 70 l/min of air. A steady output could be maintained for at least 4 hours.

For very long periods of operation Tanaka and Akiyama (1984) have a system which runs continuously for indefinite times since there is a screw feed to replenish the bed.

Aerosol formation by condensation has frequently been employed using generators deriving from the original design developed during the war at Columbia University, New York (Sinclair and La Mer 1949). It was some years until the way in which it worked was really understood. With most substances it was necessary to cool a mixture of air or nitrogen, vapour and nuclei to form aerosol particles upon the nuclei. Sulphuric acid vapour is self-nucleating (La Mer *et al.* 1950).

Muir (1965) described the sequence of aerosol formation, by the condensation of high-molecular-weight organic vapours in the cooling tube, and the existence of a radial distribution of particle size with the larger particles in the centre of the tube. The importance of avoiding convection currents became obvious and so was the need for a controlled supply of nuclei.

Swift (1967) followed up this work, trying various substances as nuclei. Sodium chloride and silver chloride were good and, for high-molecular-weight organic vapours apiezon grease was best since it dissolved in the condensate. It was found that the nuclei could be controlled by evaporating the nucleating substances from an evenly coated,

moderately heated platinum wire; up to 10 nuclei per cm^3 were obtainable. The best nuclei were 20 to 40 nm in diameter. The best aerosol substance for use in this generator was di-2-ethylhexylsebacate (DEHS). This substance has a sufficiently low vapour pressure to given an aerosol of 0·5 μm-diameter particles a working life of about an hour and can be of some use for particles as small as 0·2 μm before loss by evaporation becomes troublesome. It is not subject to thermal decomposition in the evaporator and is non-toxic so that inhalation experiments can be performed.

A number of variations in the design of this type of generator have been described and are referred to by Kerker (1975) in his review. It is not apparent that additional complication really results in a better degree of homogeneity than can be obtained when a few important modifications to the original Sinclair–La Mer have been made. They are: downwards flow of condensing vapour; controlled supply of nuclei; withdrawal of aerosol from the centre of the condensation tube; low rate of flow; uniform temperatures in the evaporator and reheater flasks, which is ensured by having them in separate insulated enclosures and distributing thermostatically controlled heating elements over their surfaces.

Stahlhofen *et al.* (1975), using DEHS with sodium chloride nuclei, obtained particles up to 4 μm diameter at a boiler temperature of 220°C, a nitrogen flow of 0·5 l/min and a nucleus concentration of $1{\cdot}8 \times 10^6\,cm^{-3}$. The geometric standard deviation ((σ_g, equation (17)) for droplets of DEHS was 1·034 for diameters 0·7 to 0·3 μm, rising to 1·06 at 0·15 μm. The size distributions of the nuclei were nearly lognormal with diameters 0·01 to 0·1 μm.

6. Particle size and size distribution

Much applied aerosol science is carried out with dust particles, large enough (above 0·5 μm diameter) to be counted and sized by optical microscopy, which have been sampled and deposited on glass slides without a mounting medium. The sizing classifies them by projected area diameters of the images which are reduced by eye to circles of the same area. This is the definition of 'projected area diameter', d_p (Davies 1979 b). It says nothing about the thickness of the particles and often relates to particles in preferred orientation, especially for particles larger than a few microns. Microscopic sizing is performed with an eyepiece graticule (Davies 1954, May 1982, Cheah 1983).

Various formulae have been used to express the size distribution of aerosols. The lognormal is of wide application and is particularly easy to use (Aitchison and Brown 1963):

$$dN/d(\ln r) = \{N/[\sqrt{(2\pi)}(\ln \sigma_g)]\} \exp[-\tfrac{1}{2}\{\ln(r/r_M)/\ln \sigma_g\}^2] \qquad (17)$$

where $N\,cm^{-3}$ is the concentration by number, r_M is the median radius and σ_g is the geometric standard deviation. When σ_g is less than 1·2 the aerosol is regarded as fairly homogeneous.

This distribution was first used for particles by Hatch and Choate (1929) who give some useful expressions derived from equation (17). The distribution, when plotted as frequency against log diameter, is symmetrical and the same as the Gaussian error curve. To show measured size distributions it is best to plot the cumulative percentages of particles up to a series of sizes. The number of particles up to size r is

$$N_r = 50[1 + \mathrm{erf}\{\ln(r/r_M)/\sqrt{2}\ln \sigma_g\}] \qquad (18)$$

It is possible to fit almost any complex, experimentally determined size distribution by a number of lognormal ones, with selected values of r_M and σ_g (Davies 1974 b, Heintzenberg 1975).

Using a log scale for r and a normal probability scale for the percentages of particles below a series of sizes, a straight-line plot is obtained, if equation (17) is obeyed, with a slope related to σ_g. Quite often the line is straight over a limited range of sizes, but the use of log-probability paper is the best way of plotting measurements.

Distributions by number, surface area, or mass, plot as parallel lines.

Another distribution formula, which is often used for spray droplets, is that due to Rosin and Rammler (1933):

$$\frac{1}{V}\int_0^{d/d_M} dV = 1-\exp\left[-0{\cdot}693(d/d_M)^b\right] \tag{19}$$

where V is the volume fraction of drops in sizes below diameter d; d_M is the volume median diameter, and the constant b is usually between 1·5 and 3. Methods of using this distribution are described by Bailey *et al.* (1983).

Power-law distributions have been discussed by the writer (Davies 1964) (see figure 13).

A self-preserving size distribution which remains of the same form while a non-homogeneous aerosol is losing particles by sedimentation has been described by Lidwell (1946). Attempts to account for the Junge type distribution, equation (14), as an example of a self-preserving form have not been entirely successful (Liu and Whitby 1968).

7. Dynamics of aerosol particles

A spherical particle falling through air of viscosity, η, encounters a drag or resistance, W, given within 5% by Stokes's law (cf. p. 145)

$$W = 6\pi a\eta v \tag{20}$$

provided that the radius, a, is between 1·5 and 30 μm; v is the velocity of the particle. More details are tabulated by Davies (1947). Above 30 μm radius the drag is greater, due to the motion induced in the air becoming sufficient to involve its inertia. Below 1·5 μm air begins to act as a discontinuous medium since the particle becomes comparable in size with the mean free path of the air molecules and the drag is less than is given by equation (20) (see equation (31)).

When (20) is valid the equation of motion in one dimension of a particle of mass m, moving at velocity v in air moving at velocity V is

$$m\,dv/dt = 6\pi a\eta(V-v) \tag{21}$$

If the acceleration is g, due to gravity, and the motion is a vertical fall through air at rest, the particle accelerates to a constant terminal velocity, v_s, given by

$$(m-m')g = 6\pi a\eta v_s \tag{22}$$

where m is the mass of the particle and m' that of the air which it displaces. Hence,

$$\tfrac{4}{3}\pi a^3(\rho-\sigma)g = 6\pi a\eta v_s \tag{23}$$

ρ being the density of the particle and σ that of air, and

$$v_s = 2a^2(\rho-\sigma)g/9\eta \tag{24}$$

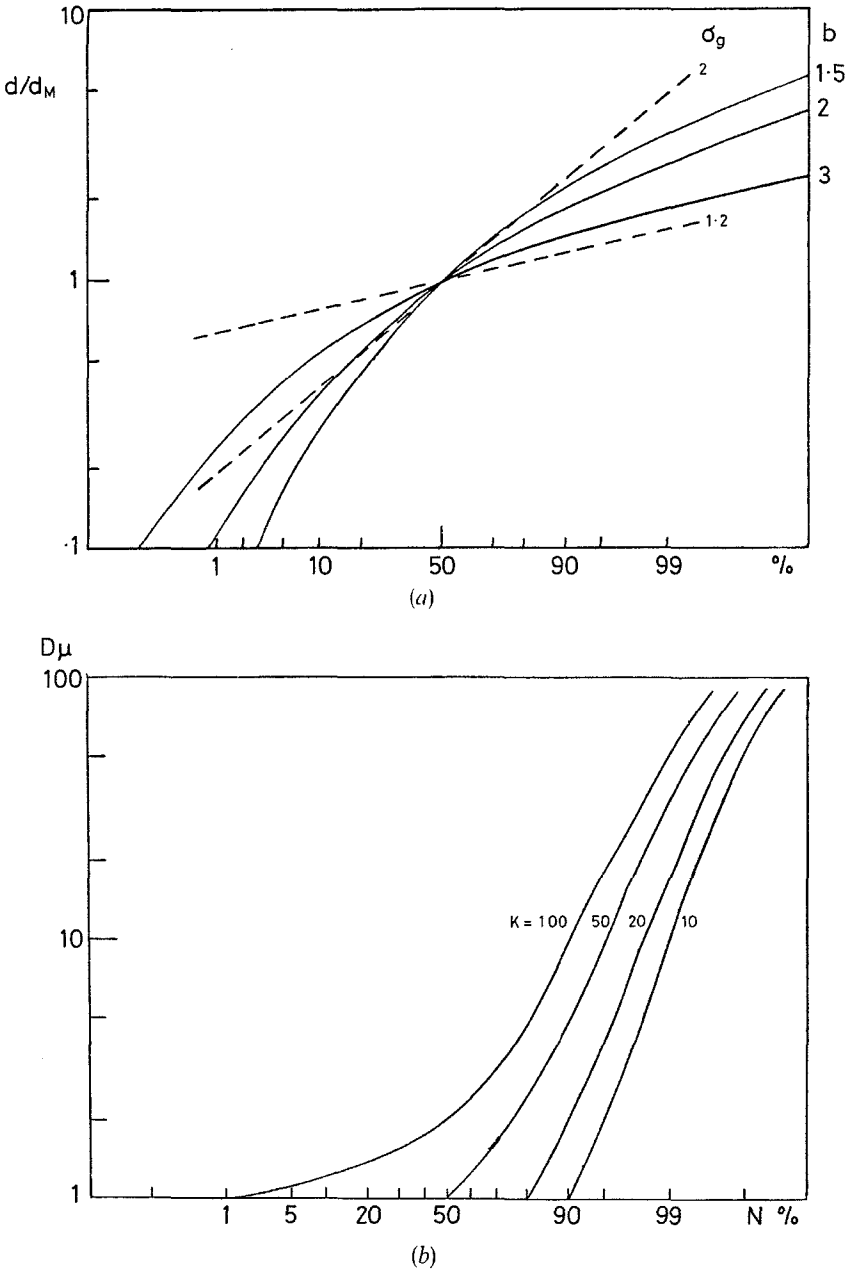

Figure 13. Particle size distributions. (*a*) Cumulative frequency distributions plotted on lognormal paper; d_M is the median particle diameter. The broken straight lines are lognormal distributions with $\sigma_g = 1{\cdot}2$ and 2·0 (equations (17) and (18)). The continuous curves are Rosin–Rammler distributions, equation (19), with $b = 1{\cdot}5$, 2 and 3. (*b*) Power law ($dN/dd = Kd^{-\gamma}$) distributions plotted on lognormal paper as cumulative curves for $\gamma = 2$. The maximum size of particle is 100 μm for each curve but by varying K the smallest particle size, $K/100$, which is included has been varied and the curves correspond to the percentages of particles above 1, 0·5, 0·2 and 0·1 μm respectively. This illustrates the change in the distributions which would be realized by counting particles with microscopes of which the resolving power improved towards the right-hand curves (Davies 1964 (*Nature*), Cartwright 1964).

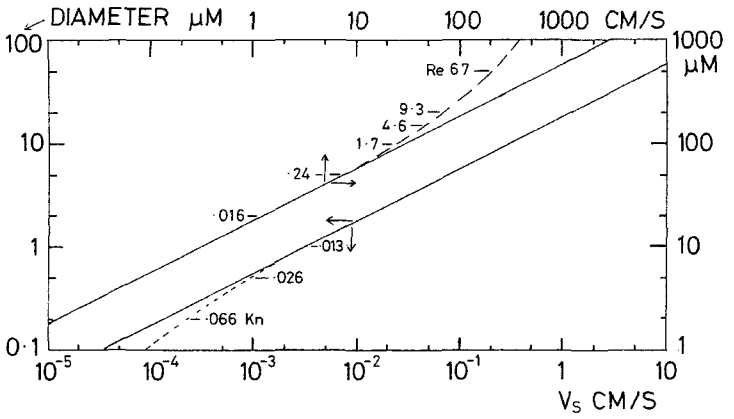

Figure 14. Falling velocities in air of spheres of unit density at 20°C and one atmosphere. Stokes's equation (24) is represented by the parallel lines. The deviation from the lower line, which raises v_s, is due to the Cunningham etc. factor F (equation (31)). The deviation from the upper line, decreasing v_s, is due to the inertial drag of air set in motion by the falling particle and is calculated by equation (30) for Re less than 4. Values of Re are shown on the upper curve and of F on the lower curve.

Usually, σ is negligible compared with ρ, in which case, putting

$$\tau = m/6\pi a\eta = 2a^2\rho/9\eta, \tag{25}$$

shows that

$$v_s = \tau g \tag{26}$$

where τ is the relaxation time of the particle/fluid system for Stokes's law drag (see equation (16)).

The character of the flow past a spherical particle moving through air changes when the Reynolds number rises above 0·4 and the drag is no longer given by equation (20). The terminal volocity, in air at 20°C and atmosphere, of a sphere of unit density and radius 30 μm is 10·7 cm/s and the Reynolds number is

$$Re = 10{\cdot}7 \times 60 \times 10^{-4}/0{\cdot}15 = 0{\cdot}43 \tag{27}$$

where 0·15 cm^2/s is the kinematic viscosity of air at 20°C.

For higher values of Re the drag is no longer proportional to the velocity of the particle, as in equation (20), but is greater; it cannot be expressed by a simple fluid mechanical formula, extending the range of Stokes's law, but depends on an experimentally established relationship between the Reynolds number, vd/ν, and the drag coefficient

$$\psi = W/\pi a^2 \cdot \tfrac{1}{2}\sigma v^2 \tag{28}$$

Since both Re and ψ contain the velocity, which is usually what is wanted, the velocity is eliminated between Re and ψ by using

$$\psi Re^2 = 8W/\pi\sigma\nu^2 \tag{29}$$

where $W=(m-m')g$, as before. The falling velocity can then be calculated, using the

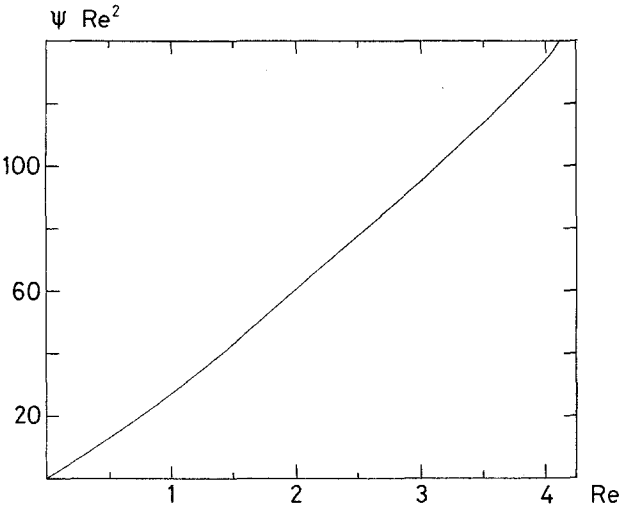

Figure 15. ψRe^2 against Re (equation (30)).

relation (Davies 1945)

$$Re = \psi Re^2/24 - 2{\cdot}363 \times 10^{-4}(\psi Re^2)^2 + 2{\cdot}0154 \times 10^{-6}(\psi Re^2)^3 - 6{\cdot}9105 \times 10^{-9}(\psi Re^2)^4 \quad (30)$$

to calculate Re, using ψRe^2 from (29) and then obtaining v from the value of Re. This procedure is valid for Re below or equal to 4, that is ψRe^2 below 140. This corresponds to a limit of 71 μm radius for a sphere of unit density in air.

Small particles, below 1·5 μm radius, are dealt with by multiplying the right-hand side of equations (24) and (25), or by dividing the right-hand side of (20), by the Cunningham–Knudsen–Weber–Millikan factor (Davies 1945, Jennings 1987)

$$F = 1 + Kn[1{\cdot}257 + 0{\cdot}400\exp(-1{\cdot}10\,Kn^{-1})] \quad (31)$$

where Kn, the Knudsen number is the mean free path of the gas molecules divided by the radius of the particle, λ/a.

A remarkable feature of aerosol dynamics is that whereas the motion of particles relative to the suspending gas is usually viscous, at low Reynolds numbers, the gas can often be treated as if it changed from a viscous fluid to an ideal one as soon as attention is focused upon the solid boundaries which contain the flowing aerosol.

This is because many problems are concerned with the impaction of aerosol particles and this needs high flow velocities; over much of the flow field the Reynolds number with respect to the flow boundaries is large. This is not the case in filters where high air speeds may result in the particles penetrating the filter because they bounce off the fibres.

It is rarely possible to solve directly the equation of motion of a particle in a complex flow field; hence recourse is necessary to the calculation of many particle trajectories, each as series of small steps. This is a slow process and it has been going on for a long time. Davies and Aylward (1951) studied the performance of impactor sampling systems in this way; 30 years later, a three-day conference, 'Gas-borne

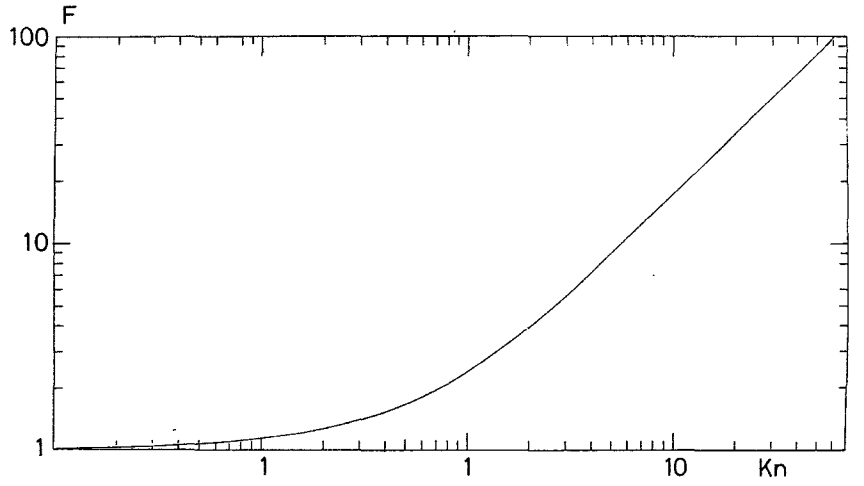

Figure 16. The Cunningham–Knudsen–Weber–Millikan drag factor, F (equation (31)), air at one atmosphere, mean free path, $\lambda = 0{\cdot}066\,\mu m$.

particles', was arranged by the Institution of Mechanical Engineers (1981) at Oxford in which a number of papers were devoted to the tracing of particle trajectories by similar methods in a variety of situations including erosion by particles in gas turbines and air compressors, the capture of gas-borne particles by baffles, and so on.

In the previous discussion the particles have been regarded as spherical. Particles of irregular but compact shape behave similarly to spheres and can be defined, as regards dynamical behaviour, by the dynamical shape factor,

$$\kappa = \frac{\text{(drag of a particle at a given velocity)}}{\text{(drag of sphere of same volume at same velocity)}} \tag{32}$$

In general, κ varies with the orientation of the particles but it is not definably associated with the geometry of the particles.

Geometrically, the size of a particle can be defined by

$$\phi_v, \text{ the diameter of a sphere of the same volume.} \tag{33}$$

Of dynamical significance is the Stokes's diameter,

$$\phi_{st}, \text{ the diameter of a sphere which has the same density and the same falling velocity as the particle,} \tag{34}$$

and

$$\phi_{ae}, \text{ the aerodynamic diameter, that is the diameter of a sphere of unit density (g/cm}^3\text{) which has the same falling velocity as the particle and } \phi_{ae} = \phi_{st}\rho^{1/2}. \tag{35}$$

The falling velocity of a particle is thus, by (24) and (34),

$$v_s = \phi_{st}^2 \rho g / 18\eta \tag{36}$$

provided that $v_s\,\phi_{st}/\nu$ is less than 0·43, equation (27), and assuming that the particle is much denser than air. For small particles alternatively, Kn must be less than 0·04.

For such particles the drag at the terminal velocity, v_s, is

$$mg = \tfrac{1}{6}\pi\phi_v^3\rho g \tag{37}$$

and the drag of a sphere of the same volume is

$$3\pi\phi_v\eta v_s \tag{38}$$

Hence, by (32), (37) and (38), the dynamic shape factor,

$$\kappa = \phi_v^3\rho g/18\phi_v\eta v_s$$
$$= \phi_v^2\rho g/18\eta v_s \tag{39}$$

which, by (36) gives

$$\kappa = \phi_v^2/\phi_{st}^2 \tag{40}$$

Values for various kinds of particles of the dynamic shape factor and the different diameters will be found in the paper by Davies (1979 b). These quantities are important in characterizing the behaviour of airborne dust particles.

The discussion in this section has hitherto related to the steady motion of particles. At low Reynolds numbers the drag is given by equation (20) for both accelerating and steady motion. This is no longer the case when the drag is not proportional to the velocity but has to be determined from the drag coefficient, ψ, equation (28). Approximate calculation of accelerating trajectories is often carried out by assuming that the drag is simply a function of the velocity, regardless of its not being constant. This can lead to errors, but the true situation is liable to be very complicated and the experimental basis which exists for steady motion is lacking for acceleration.

8. Brownian motion and diffusion of particles

Brownian motion of aerosol particles is commonly described as being the result of their bombardment by molecules of gas. This is not accurate; motion is intrinsic in the particles just as the gas molecules are themselves in thermal motion.

From the Maxwellian distribution of the velocities of gas molecules, the mean molecular velocity at temperature T is

$$\bar{v} = (8kT/\pi m)^{1/2} \tag{41}$$

where k is Boltzmann's constant ($1{\cdot}381 \times 10^{-16}$ erg/K) and m is the mass of a molecule of gas of molecular weight M_w.

$$m = 1{\cdot}661 \times 10^{-24} M_w \tag{42}$$

On Maxwell's idea of equipartition of energy the mean thermal velocity of an aerosol particle of mass M in equilibrium with the gas is given by equation (41) as

$$\bar{V} = (8kT/\pi M)^{1/2} \tag{43}$$

This is the mean velocity of the Brownian motion of the particles.

Note the equivalence of the thermal energy of the molecules of gas and of the particles suspended in the gas to form an aerosol. From (41) and (43)

$$m\bar{v}^2 = M\bar{V}^2 = 8kT/\pi = 2{\cdot}547kT \tag{44}$$

so the heavier the particle, the less is its Brownian motion.

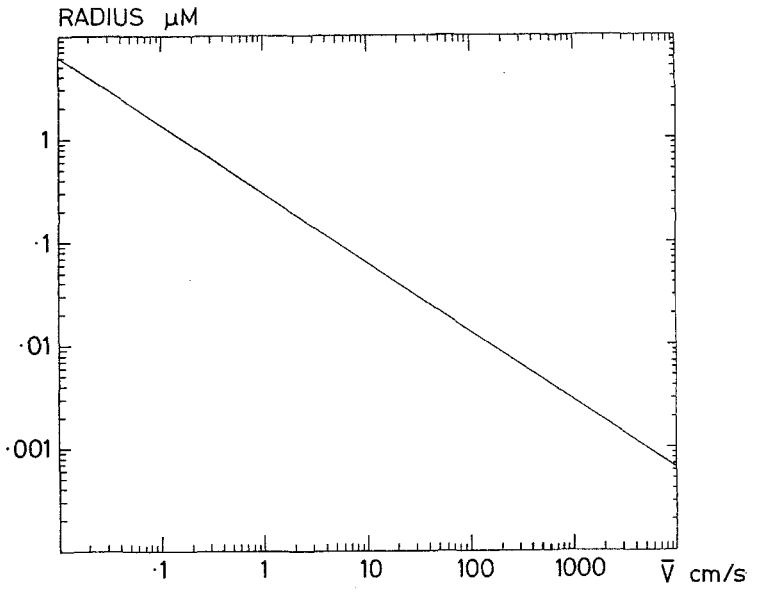

Figure 17. The mean thermal velocity of aerosol particles of unit density at 20°C (equation (43)).

Because both gas molecules and suspended particles are in motion, with the above mean velocities, they diffuse when in contact with another gas, the reason being the need to eliminate differences of concentration and to raise the entropy of the system. The rate of diffusion is proportional to the concentration gradient of the molecules or the particles, and the constant of proportionality is defined as the coefficient of diffusion, D.

The coefficient of gas diffusion is calculated by kinetic theory. The elementary formula is

$$D=\tfrac{1}{3}\lambda\bar{v} \tag{45}$$

When two gases are placed in contact their molecular velocities cause mixing by interdiffusion, according to their respective diffusion coefficients, which have to be equal to avoid the creation of a pressure difference:

$$D_{12}=D_{21} \tag{46}$$

Meyer's formula for the interdiffusion of gases 1 and 2 is

$$D_{12}=D_{21}\frac{n_1\bar{v}_2\lambda_2+n_2\bar{v}_1\lambda_1}{3(n_1+n_2)}\text{cm}^2/\text{s} \tag{47}$$

where the ns are concentrations of molecules, the λs are the mean free paths for each gas and the $\bar{v}$s are the mean thermal velocities (41). This formula exaggerates the dependence of D upon the concentrations.

If the gases are similar, (47) reduces to (45), but if correction is made for persistence of velocities after collision it becomes, more accurately,

$$D=\lambda\bar{v}/1{\cdot}78 \tag{48}$$

If gas 2 is replaced by aerosol particles, then n_2 is much smaller than n_1; hence from (47),

$$D_{21} = \lambda_2 \bar{V}_2 / 1{\cdot}78 \tag{49}$$

λ_2 can be identified with the stop-distance of a particle $F\tau\bar{V}_2$, since collisions between particles are relatively rare. Hence the coefficient of diffusion of particles into the gas is

$$D = F\tau\bar{V}^2/1{\cdot}78 \tag{50}$$

This makes the diffusion coefficient of particles too large. It is better to calculate it from Einstein's equation which equates diffusive transport of particles to that produced by a force acting on the particles,

$$D = kTB \tag{51}$$

where B is the mobility of the particle, that is, the velocity produced by unit force acting against the drag of the particle. For spheres,

$$B = \tfrac{1}{6}vF/\pi a\eta v = \tau F/m \tag{52}$$

using (25) and now using m as the mass of the particle and v, which cancels, for its

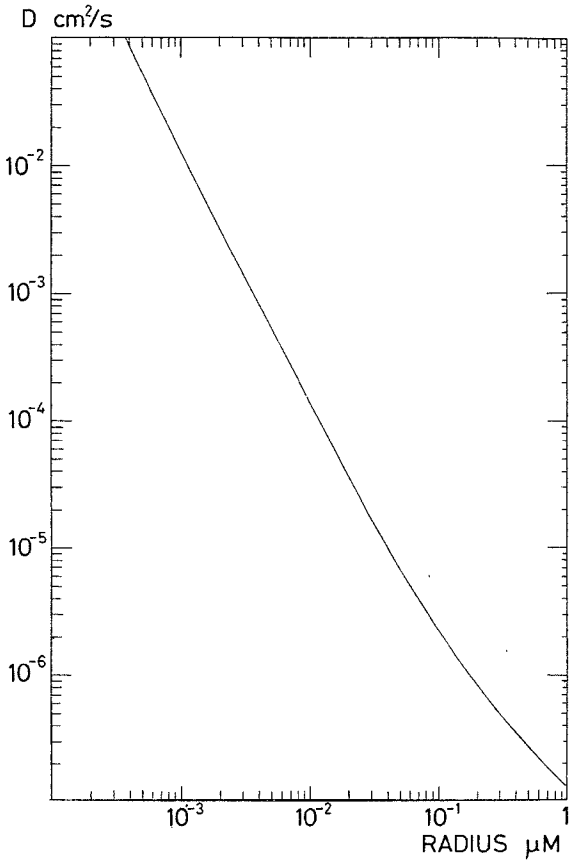

Figure 18. The diffusion coefficient of aerosol particles of unit density in air at 20°C and one atmosphere (equation (54)).

velocity. Note that diffusion is important mainly for small particles so the Cunningham etc. factor, F equation (31) is essential.

In calculating the pressure produced by a gas from kinetic theory, it is shown, independent of the distribution of velocities, that (compare with equation (44)),

$$\tfrac{1}{2}mv^2 = \tfrac{1}{2}3kT \tag{53}$$

which implies three translatory degrees of freedom but no rotation. Combining the last three equations, we obtain, for particles,

$$D = \tfrac{1}{3}\overline{V^2}\tau F \tag{54}$$

The particle relaxation time, τ, is given by equation (25). This result should be compared with equation (50). From kinetic theory,

$$\overline{V^2}/\bar{V}^2 = 1{\cdot}178 \tag{55}$$

Comparing equations (50) and (54),

$$D_{54} = \tfrac{1}{3}D_{50} \times 1{\cdot}78 \times 1{\cdot}178 = 0{\cdot}699D_{50}$$

Experimental determinations of the coefficient of diffusion of particles have been discussed by Fuchs (1964, p. 193). Some of them, plus the agreement of measured coagulation rates with theory based on diffusion, support the accuracy of equation (54). In addition, the continuity of the transition from the diffusion of high-molecular-weight gas molecules to the diffusion of small particles has been illustrated by the writer (Davies 1985).

9. Coagulation

The understanding of coagulation started with the classical paper of Smoluchowski (1917) which was directed at colloidal solutions and the association of their colour changes over time with an increasing size of the particles, due to coagulation. The motion of the particles which resulted in collisions between them was identified as their Brownian motion.

With this picture in mind, he calculated the diffusion of surrounding particles towards a single, temporarily fixed particle of the same radius, a, as the diffusing ones; at the surface of the fixed particle the concentration was zero since contact with it resulted in adhesion. By solving the diffusion equation with spherical symmetry, he calculated the total diffusion inflow up to time, t, and showed that any particle in volume V would have a probability of colliding with the central particle during time, t, which was equal to

$$W_t = (4\pi Da/V)\{t + 2a\sqrt{t}/\sqrt{(\pi D)}\} \tag{56}$$

A steady state ensues after a time great compared with a^2/D which, in fact, is a very short time. Hence, the probability of a collision between a mobile particle and the fixed, central one, in unit time is

$$W = 4\pi Dav_0 \tag{57}$$

where v_0 is the initial number of particles per unit volume.

Suppose that every particle is active as a centre of condensation, but each acts independently of the others.

The number of particles left after time t is

$$v_1 = v_0 \exp(-4\pi D a v_0 t) \tag{58}$$

or,

$$dv_1 = 8\pi D a v_0 v_1 \, dt \tag{59}$$

where the right-hand side has been doubled to allow for the central particle, towards which diffusion has been calculated by (57), being itself in motion. The equation for coagulation of uniform spheres is therefore

$$dv/dt = -8\pi a D v^2 \tag{60}$$

which defines the coefficient of coagulation, K

$$K = 8\pi a D \tag{61}$$

Since aD is independent of the radius of the particles (equations (51) and (52)), the rate of rapid coagulation of particles in a colloidal solution is independent of their size, apart from the drag factor, F, which is unity in liquid suspensions. This is not so for aerosols. From equations (51) and (52) the diffusion coefficient of aerosol particles is

$$D = (kT/6\pi\eta)(F/a) \tag{62}$$

so that the coefficient of coagulation of aerosol particles is (for $Kn < 13$, see equation (68))

$$K = (4kT/3\eta)F \tag{63}$$

The drag factor is thus extremely important for aerosols; it can be seen from equation (31) that F increases steadily as Kn increases so that in air at constant pressure the coagulation coefficient would also have to rise indefinitely. This is not possible; if the particles were to decrease in size until they approached gas-molecular dimensions, the coagulation coefficient would have to come into line with the molecular collision frequency as calculated by kinetic theory.

Jeans (1925, p. 37) shows that the number of collisions between gas molecules per unit volume is

$$\pi v^2 4a^2 \bar{v}/\sqrt{2} \tag{64}$$

where a is the radius of the molecules, $\bar{v}$ their mean velocity and v the number of molecules per unit volume. If the molecules were to adhere on collision this would give an equation analogous to (60):

$$dv/dt = -\pi 4a^2 \bar{v} v^2/\sqrt{2}$$

making

$$\begin{aligned} K_{gk} &= \pi 4a^2 \bar{v}/\sqrt{2} \\ &= (48akT/\rho)^{1/2} \end{aligned} \tag{65}$$

which is independent of Kn.

K_{gk} is the gas-kinetic coefficient of coagulation which can operate only at very high values of the Knudsen number, Kn. This means that it can be realized only at pressures well below one atmosphere; otherwise, particles of impossibly small radii would be needed to obtain the high values of Kn (table 4).

Table 4. The gas-kinetic coefficient of coagulation, K_{gk} (equation (65)), calculated for spheres of unit density at 20°C.

a (cm)	$\bar{V}$ (cm/s)	K_{gk} ($cm^3 s^{-1}$)	Kn	$10^6\lambda$ (cm)	Pressure (cm Hg)
10^{-7}	4957	$4{\cdot}40\times10^{-10}$	110	11	45·6
10^{-6}	156·8	$13{\cdot}9\times10^{-10}$	47	47	10·7
10^{-5}	4·96	$41{\cdot}1\times10^{-10}$	29	290	1·73
10^{-4}	0·157	$139{\cdot}5\times10^{-10}$	29	2900	0·173

The curve of the variation of the coagulation coefficient against Kn rises with increasing Kn from $Kn\sim0$, following equation (63). But with falling Kn, below a high value, say $Kn=100$, the value of K also rises. It is thus obvious that at some intermediate value of Kn the coagulation coefficient must pass through a maximum.

The situation was explained by the writer (Davies 1979 a) who reviewed previous measurements of K, none of which had been carried out at values of Kn exceeding 25. Many of the previous results were inaccurate for various reasons. Additionally, current theoretical predictions were impossible since they tended to introduce the gas-kinetic concept at quite small values of the Knudsen number.

An experimental programme was therefore launched for the measurement of the coefficient of coagulation at much higher values of the Knudsen number. The first experiments by Rooker and Davies (1979) confirmed, along with the better of the preceding experiments, that equation (63) was valid up to $Kn=13$ which, at atmospheric pressure, required particles of 5 nm radius. Further experiments were carried out with smaller particles (Egilmez and Davies 1982, 1986) which showed that the maximum value of the coagulation coefficient was near to $K=105\times10^{-10}\,cm^3\,s^{-1}$ at $Kn=23$. The highest value of Kn attained was 42 with particles of 1·6 nm radius.

It was shown by Davies (1979 a) how a factor, β_D, could be deduced to multiply the coefficient of coagulation, as defined by equation (63), and would interpolate smoothly between equation (63), which can be termed the Smoluchowski–Cunningham–Knudsen–Weber–Millikan regime, and the gas-kinetic regime of equation (65). With the latest results available this factor, with the same form as proposed in 1979, could have its single arbitrary constant evaluated by fitting to the experimental results. Hence,

$$\beta_D=[1+Pe^{-1}+4\sqrt{2}\exp(-25Pe)]^{-1} \tag{66}$$

where

$$Pe=2\bar{V}a/D \tag{67}$$

D is given by equation (62) and $\bar{V}$ by (43).

With decreasing Kn the value of β tends to unity at $Kn=17$. The value of the coagulation coefficient is now experimentally established as

$$K=4kTF\beta_D/3\eta \tag{68}$$

for Kn smaller than 42.

There is no experimental backing for equation (68) above $Kn=42$. However, the value it gives for K at $Kn=115$ is very close to K_{gk}, $3{\cdot}4\times10^{-10}\,cm^3/s$ for particles of calcite (density 2·7 g/cm³) at 20°C, radius 6×10^{-8} cm. The course of the K versus Kn curve is shown on figure 19.

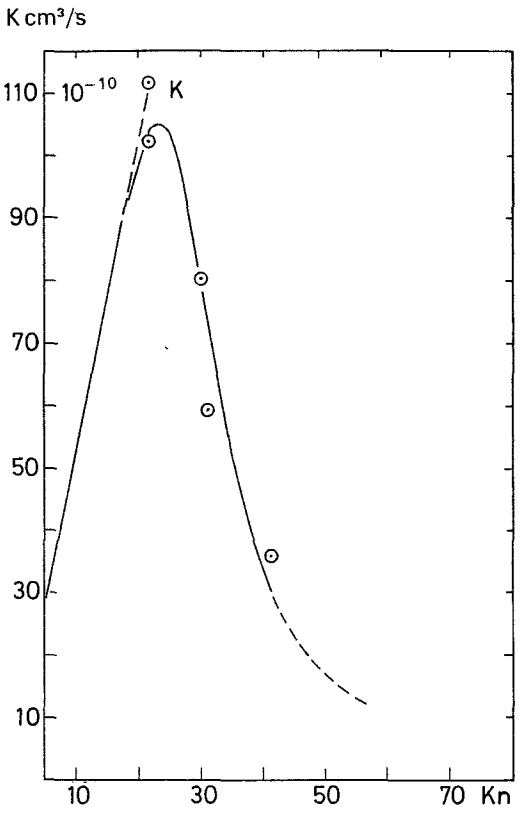

Figure 19. The coagulation coefficient of aerosols of particles of calcite (2·7 g/cm^3) in air at 20°C and one atmosphere. Curve calculated by equation (68) and experimental points from Egilmez and Davies (1986).

Before Smoluchowski's coagulation theory, it had been observed by Wiegner (1911) that in colloidal solutions the rate of loss of small particles was enhanced if larger particles were added. This is not difficult to understand. If a given concentration of small particles were to have some of them replaced by larger ones the total surface area of the particles would be increased and with it the rate of coagulation. This is a convenient phenomenon in one respect. The rate of decrease in number of particles, dv/dt (equation (60)), would decrease with time as the number concentration diminished with the result that the familiar straight-line plots of $1/v$ against time would curve downwards.

In fact, the lines do appear to stay straight for longer times than would be expected, which is probably due to the Wiegner effect.

Some experiments were carried out on mixed aerosols by Egilmez and Davies (1986) in which an aerosol of fine particles, $r_F = 1{\cdot}6\,\text{nm}$, was mixed with one of coarse particles, $r_c = 0{\cdot}25\,\mu\text{m}$. The diffusion coefficient of the fine particles, $D_F = 5{\cdot}05 \times 10^{-3}\,\text{cm}^2/\text{s}$, was over 8000 times larger than that of the coarse. The concentrations were n_F and $n_c\,\text{cm}^{-3}$.

Coagulation of fine particles with fine arises from pairs of particles diffusing into contact, so the coefficient of coagulation (equations (61), (63) and (66)) is

$$K_F = 2\pi \cdot 2r_F 2D_F \beta_D \tag{69}$$

in which $2r_F$ is the distance between particle centres when in contact and $2D_F$ is the diffusion coefficient of their mutual approach.

Coagulation of fine particles with a coarse particle is the result, not of their mutual approach, but of the diffusion of fine particles to a virtually stationary coarse one, since r_c is large enought for the thermal motion to be negligible. As a result, the coagulation coefficient of fine particles with coarse is

$$K_m = 2\pi r_c D_F \tag{70}$$

since r_F is negligible compared with r_c, and D_c is negligible compared with D_F. This equation agrees with equation (49.26), p. 294 of Fuchs (1964) apart from his erroneous β. The factor, β_D, is not required in (70) since the collision frequency of small particles with a large one is independent of the partitioning of the thermal energy of the small particles between the directed and random fractions (Davies 1979 a).

The rate of loss of small particles by mutual coagulation plus their coagulation with coarse particles is

$$-dn_F/dt = Kn_F^2 + K_m n_F n_c \tag{71}$$

where n_c is constant. However, there is also a loss of small particles by diffusion to the walls of the container; this is represented by Ln_F where L is defined as the fraction of all the particles in the container that is lost to the walls per second. Thus, n_F in (71) represents the true number of small particles per cm^3 at time t and

$$-dn_F/dt = Kn_F^2 + (K_m n_c + L)n_F \tag{72}$$

The loss of coarse particles is negligible. Integrating (72):

$$-t = \int_0^{n_t} \frac{dn_F}{Kn_F^2 + (K_m n_c + L)n_F} \tag{73}$$

since n_c is constant, n_t is the concentration of fine particles after time t.

$$-t = \frac{-2}{K_m n_c + L}\left[\coth^{-1}\frac{2Kn + K_m n_c + L}{K_m n_c + L}\right]_0^{n_t}$$

giving

$$\exp\{-(K_m n_c + L)t\} = \frac{n_t}{n_0} \cdot \frac{Kn_0 + K_m n_c + L}{Kn_t + K_m n_c + L}$$
$$= f(n_t) \tag{74}$$

Experiments were carried out to test this equation with three different concentrations of coarse particles. The concentrations of fine particles were measured at intervals of about 200 s, giving values of n_t which decreased to about a quarter of the initial value in 800 s. Experimental values of $f(n_t)$ are plotted against $\exp\{-(K_m n_c + L)t\}$ on figure 20.

The experimental points lie along the line of equation (74) for short times (exponential above 0·4) but tend to larger values of $f(n)$ as time increases beyond 400 and 600 s. This may be due to the smaller particles in the near homogeneous aerosol being removed preferentially in the early stages of coagulation.

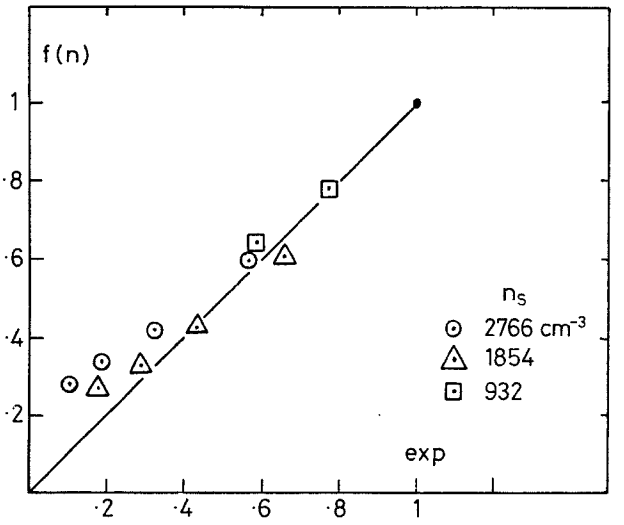

Figure 20. Coagulation of mixed aerosols (particles 1·6 nm radius and particles of 0·25 μm radius). The line is theoretical, equation (74); the experimental points are from Egilmez and Davies (1986).

10. Evaporation and condensation

For aerosols to have a long life they need to be composed of particles of low volatility and the smaller the particles the lower their vapour pressure must be. In a review by the writer (Davies 1978) it is shown how evaporation may be controlled either by the diffusion of volatile molecules away from the particle or, when the diffusive transfer is theoretically very rapid, by surface resistance to the escape of molecules which need not imply the presence of a surface film.

Very small droplets tend to evaporate more rapidly per unit area of surface, because of the raising of the vapour pressure by the curvature of the surface. For a droplet of radius a the vapour pressure, p_a, divided by the normal vapour pressure, p, is

$$p_a/p = \exp(2\gamma M/R_M T a\rho) \tag{75}$$

where M is the molecular weight of the vapour, ρ the density and γ the surface tension of the liquid, R_M the gas constant per mole and T the absolute temperature.

The Kelvin effect (equation (75)) is rarely important for diameters above 1 μm. It shows that when a is very small, the equilibrium vapour pressure is much larger than the standard value, p, so that growth by condensation on hygroscopic nuclei is much retarded (table 2) for diameters below d_{min} of equation (4), which is the same as (75). The validity of the equation has been confirmed by experimental tests (Skinner and Sambles 1972).

The simplest case of evaporation is that of spherical droplets of a pure substance which, when its saturation vapour pressure is fairly low, is isothermal since latent heat cooling is small and is eliminated by conduction from the surrounding air. With small drops a pseudo-steady state is rapidly established so that the drop size changes slowly and the distribution of vapour concentration runs from saturation at $r=a$ to zero or some constant value at a distance.

If c is the vapour concentration at a distance r from the centre of the drop, the diffusion equation reduces to

$$\frac{2}{r}\frac{dc}{dr}+\frac{d^2c}{dr^2}=0 \tag{76}$$

Hence,

$$dc/dr=-A/r^2 \tag{77}$$

The rate of loss of weight by a droplet of radius a is given by Fick's law as

$$\dot{m}=4\pi a^2 D(dc/dr)_a \tag{78}$$

giving, by (77),

$$A=-\dot{m}/4\pi D \tag{79}$$

so that

$$dc/dr=\dot{m}/4\pi Dr^2 \tag{80}$$

and

$$c_a-c_\infty=(\dot{m}/4\pi D)\int_a^\infty r^2\,dr=\dot{m}/4\pi aD \tag{81}$$

Hence, the rate of evaporation, when diffusion controlled, is

$$\dot{m}_D=4\pi aD(c_a-c_\infty)\,\text{g/s} \tag{82}$$

which is Maxwell's equation; it can be converted to saturation vapour pressure, p_a and the ambient vapour pressure, p_∞, at a distance from the drop by supposing the vapour to be a perfect gas of molecular weight M, when

$$c=Mp/R_MT\,\text{g/cm}^3 \tag{83}$$

and

$$\dot{m}_D=(4\pi aDM/R_MT)(p_a-p_\infty)\,\text{g/s} \tag{84}$$

Referring back to (82),

$$\dot{m}_D=\frac{d}{dt}(4\pi a^3\rho/3)=2\pi\rho a\frac{da^2}{dt} \tag{85}$$

This is a useful equation since the rate of change of surface area is independent of the radius of the droplet so that the lifetime is easily obtained. For example, using (82),

$$da^2/dt=2D(c_a-c_\infty)/\rho=\text{constant} \tag{86}$$

ρ is the density of the condensed phase. This supposes that the concentration of involatile impurities dissolved in the drop is small enough not to reduce the vapour pressure as evaporation proceeds.

Unfortunately this simple calculation does not always work. It will be seen from (80) that the concentration gradient of vapour at the surface is inversely proportional to the square of the radius of the droplet, which demands impossibly high rates of escape of molecules from the liquid to the vapour phase for small droplets.

It is assumed that the rate of escape of molecules from the liquid is that which balances the rate of restoration of molecules from the gas to the liquid phase at saturation vapour pressure. This same rate of escape determines the rate of evaporation into a vacuum.

From kinetic theory, the number of molecules which strike the surface of the droplet when it is in equilibrium with saturated vapour is

$$\tfrac{1}{4}n\bar{v} \times 4\pi a^2, \mathrm{s}^{-1} \tag{87}$$

where $\bar{v}$ is the mean velocity of vapour molecules and n is the number of vapour molecules per cm^3 in saturated vapour.

It is possible that not all vapour molecules which strike the surface will be absorbed. A condensation coefficient, α, is therefore defined which is equal to the fraction absorbed; at equilibrium, therefore, the rate of evaporation must be

$$\alpha\tfrac{1}{4}n\bar{v} \times 4\pi a^2 \quad \text{molecules/s} \tag{88}$$

It is supposed that this rate is independent of the external pressure and thus gives the rate of evaporation into a vacuum, α now being an evaporation coefficient.

Alty and Mackay (1935) experimented with millimetre-sized drops of water, using rapid pumping to remove the vapour, and found that the evaporation coefficient was 0·036. Narusawa and Springer (1975) found $\alpha = 0{\cdot}038$ for a stationary water surface but 0·18 for a flowing surface.

A survey of the literature was made by Paul (1961) who listed values for many substances. Metals and non-polar organic compounds probably have $\alpha = 1$, the maximum possible value. He noted that experimental errors tended to result in low values of α. It was suggested that the condensation coefficient might not be the same as the evaporation coefficient, as was assumed in equation (88); in some cases evaporating molecules were not the same as condensing ones, because of association of the latter.

Evaporation of drops can be slowed by coating the surface with films of polymers. Experiments with water droplets by Eisner *et al.* (1960) showed that α could be reduced to $2{\cdot}9 \times 10^{-5}$ if they contained 0·2% of a mixture of C_{14} to C_{18} straight-chain primary alcohols.

The treatment above makes no allowance for the latent heat of evaporation which causes the particle to cool appreciably unless it has a low vapour pressure; as a result, the lifetime is longer than that obtained from equation (86), (Davies 1978). The temperature fall is independent of particle size, but requires a longer time to be established for larger particles. This is why water droplets cool to the temperature of the wet bulb thermometer.

The Knudsen number of a particle evaporating into air is defined as before when its drag was being considered (equation (31)),

$$Kn = \lambda/a$$

where λ is the mean free path of the molecules of air (0·066 μm at one atmosphere) and a is the radius of the particle.

The rate of evaporation given by equation (82) or (84) is correct for small values of Kn, and that given by equation (88) is correct when Kn is large. A method of interpolating between these situations was devised by Fuchs (1934) and is known as the flux matching method.

Suppose that the concentration of vapour at a small distance, Δ, from the surface of the drop is c_Δ. The rate of evaporation from the surface of the drop, following equation (88), is, for kinetic control,

$$\dot{m}_k = \alpha 4\pi a^2 \times \tfrac{1}{4}\bar{v}(c_s - c_\Delta) \tag{89}$$

which assumes saturation vapour concentration, c_s, at $r = a$, the surface of the drop, and concentration, c_Δ, at a distance Δ from the surface. For $r > \Delta$, transfer of vapour from the drop is by diffusion; hence, from (82),

$$\dot{m} = 4\pi(a+\Delta)Dc_\Delta \tag{90}$$

which must be equal to $\dot{m}_k$ (89). Elimination of c_Δ between the last two equations gives

$$\dot{m} = \frac{4\pi aD(c_s - c_\infty)}{4D/\alpha\bar{v}a + a/(a+\Delta)} \tag{91}$$

Here,

$$4\pi aD(c_s - c_\infty) = \dot{m}_D$$

is the diffusion controlled rate of evaporation, equation (82); putting $D/\bar{v} = \frac{1}{3}\lambda$, equation (45), we obtain

$$\dot{m} = \frac{\dot{m}_D}{\frac{4}{3}Kn/\alpha + a/(a+\Delta)} \tag{92}$$

An experimental check of this equation was carried out by Bradley *et al.* (1946) over values of Kn up to 1000. They used drops of organic compounds of low volatility around 0·5 mm diameter and varied the Knudsen number by working at pressures down to 0·1 torr. They found values of 0·28 to 0·35 for the evaporation coefficient. Both they and Davis and Ray (1978) confirmed that the rate of change of surface area was constant. The latter used sub-micron drops of dibutyl sebacate and dioctyl phthalate suspended electrically in various gases; it was confirmed that the fall in temperature was negligible. The evaporation coefficient was unity but their maximum value of Kn was below 2.

Equation (92) is not convenient to use in numerical calculations. It has been put into integrable form by the writer (Davies 1973) using the expression for the thickness of the Fuchs Δ layer given by Wright (1960).

$$\Delta = 2D/\bar{v} \tag{93}$$

Substituting for D from (45), this gives, approximately,

$$\Delta = \tfrac{2}{3}\lambda \tag{94}$$

so that

$$a/(a+\Delta) = 1/(1+\tfrac{2}{3}Kn) \tag{95}$$

and

$$\dot{m}/\dot{m}_D = [(\tfrac{4}{3}Kn/\alpha + 1/(1+\tfrac{2}{3}Kn)]^{-1} \tag{96}$$

When $Kn \to 0$ this gives $\dot{m} \to \dot{m}_D$ and when Kn is large, $\dot{m} \to \dot{m}_k$ (89), and

$$\dot{m}_k = \dot{m}_D(\tfrac{3}{4}\alpha/Kn) \tag{97}$$

Hence $\dot{m}/\dot{m}_D$ is a unique function of Kn which tends to the correct limits for small and large values of Kn.

Fuchs and Sutugin (1971) rejected an equation very similar to (96), claiming that it did not give a correct limit for large values of Kn; this was a mistake.

Instead, they used an equation based on the work of Sahni for an analogous problem in nuclear physics; by combining their equations (3.24 and 3.27) this gives

$$\dot{m}/\dot{m}_D = [1 + Kn(1{\cdot}333\,Kn + 0{\cdot}71)/(Kn+1)]^{-1} \tag{98}$$

In fact, the function of Kn on the right-hand side of this equation goes to the same limits for small and large Kn as that of (96) and there is little difference for intermediate values.

Another equation, due to Smirnov, is quoted by Davis and Ray (1978), their own equation (8). Taking $\alpha = 1$, this gives impossibly small values of $\dot{m}/\dot{m}_D$ for high values of Kn and is accordingly rejected. They also quote a more complicated equation of Bademosi and Liu (1971) which goes to the correct limits and, in place of equation (45) for the diffusion coefficient, uses $D = \beta\lambda\bar{v}$. Davis and Ray discuss the values of β which have been employed and also some more accurate kinetic theory formulae for D.

In order to calculate the decrease in size with time and the lifetimes of particles, equation (98) was transformed to give dy/dt where $y = Kn^{-1}$. This equation was then integrated giving t as a function of y up to t_∞, the lifetime.

The original paper must be consulted for details of the integrations. During evaporation, the decreasing size of the particle causes the vapour pressure rise, by the Kelvin effect (75), which is allowed for. Evaporative cooling is not allowed for. Four quantities remain constant during evaporation:

Bulk saturation vapour concentration, c_0,
Ambient vapour concentration, c_∞,
Diffusion factor, $Di = Dc_0/\rho\lambda^2, s^{-1}$,
Kelvin factor, $Ke = 2\gamma M/R_M T\rho\lambda$, dimensionless.

The maximal rate of evaporation occurs when the ambient vapour concentration, $c_\infty = 0$. The lifetime in dimensionless units is then

$$[tDi]_{vf} = \left[0{\cdot}5y_0^2 - \left(\frac{0{\cdot}623}{1-K}\right)(y_0 - \ln(y_0+1)) + \frac{1{\cdot}333 - 1{\cdot}71K + K^2}{1-K}\left(y_0 - K\ln\frac{y_0+K}{K}\right)\right] \tag{99}$$

where the suffix vf indicates the vapour-free situation and y_0 is the initial value of y.

The minimal rate of evaporation is for particles evaporating into an atmosphere saturated with vapour, purely on account of the Kelvin enhancement of vapour pressure,

$$[tDiKe]_{sat} = 0{\cdot}333y_0^3 + 0{\cdot}355y_0^2 + 0{\cdot}623y_0 - 0{\cdot}623\ln(y_0+1) \tag{100}$$

Substances of low vapour pressure tend to saturate the surrounding atmosphere with vapour, even when only a small number of particles is present. Equation (100) is required in such cases.

11. Compositional analysis

The composition of an aerosol may vary with the particle size; in this case, non-selective filter sampling would be inadequate and a multi-stage cascade impactor would be preferred. The importance of the analysis of individual particles is stressed by Spurny (1986).

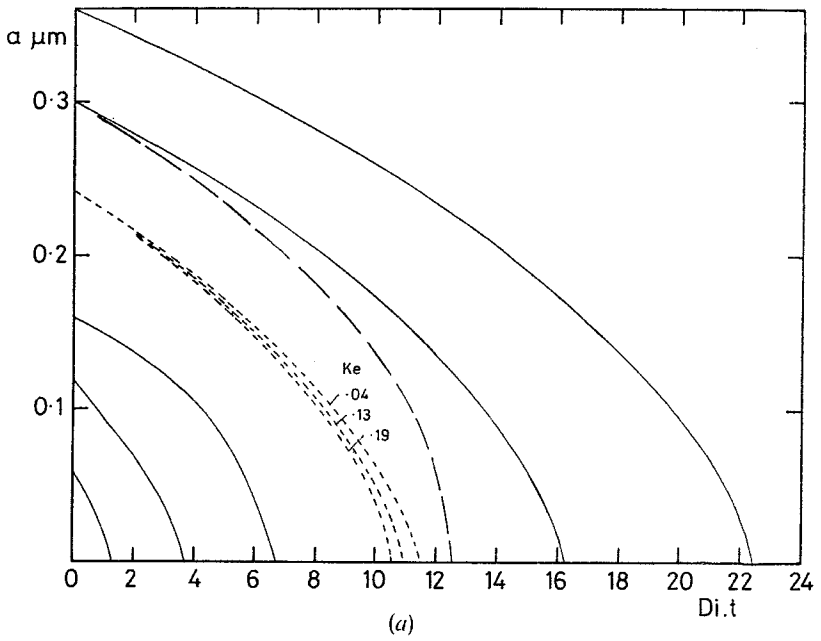

(*a*)

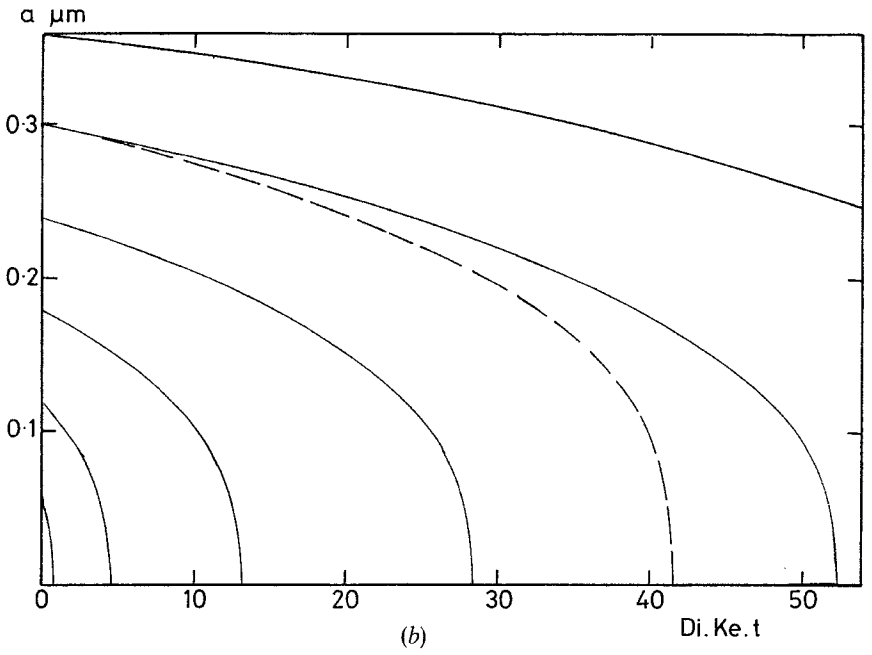

(*b*)

Figure 21. Evaporation of aerosol particles, 20°C, 1 atm., $\alpha = 1$. (*a*) Into vapour-free air. ———, $Ke = 0{\cdot}1$; - - - - - - -, $Ke = 0{\cdot}04$, 0·13 and 0·19; — —, evaporation with diffusion control. (*b*) Into vapour-saturated air; these curves are common to all substances. ———, Including the free molecular flow region near the particle; — —, calculated for $\Delta = 0$, diffusion from the surface of the particle.

Detector films for coating the impactor plates have been developed by Liddell (1947) which enable individual droplets of several liquids to be identified, down to 1 or 2 μm diameter. Water droplets down to 0·8 μm diameter can be identified when deposited on gelatine films containing naphthol green B (Liddell and Wootten 1957).

Anyz (1966) developed detector surfaces for sulphate particles; gelatine film containing barium chloride was best. After collecting the sample, the film was exposed to water vapour which developed the traces of sulphate-containing particles and suppressed those due to chloride. Waller (1963) used slides and filter paper impregnated with thymol blue to detect sulphuric acid droplets.

Bigg and Williams (1974) describe a number of chemical tests which, with the aid of electron microscopy, can identify aerosol particles weighing 10 μg or less (0·1 μm diameter). Oxidizing acid, sulphates, nitrates, persulphates and halides can be dealt with. Electron microscope grids are prepared which have been covered with films of nitrocellulose strengthened with a carbon film. Half is then shielded and the open part is exposed to reagent by vacuum evaporation. The aerosol particles are then deposited on the whole grid and exposed to vapour of water or ethyl alcohol to start the reaction; when it is complete, a film of gold–palladium alloy is evaporated over the deposit. Comparison of the two halves, under the electron microscope, enables the proportion of the deposited particles which have reacted to be determined.

Binek *et al.* (1967) obtained atomic emission spectra from individual particles, some as small as 0·02 μm diameter. Airborne particles were introduced individually into a hot chamber; if they were neither chemically reactive nor volatile a continuous spectrum was emitted and the particles can be classified by size. If evaporation occurs, a line spectrum results above the excitation temperature and elements can be identified; molecular vapour gives rise to a band spectrum. Some degree of chemical as well as size analysis can thus be achieved. More recently, Binek (1970) has used a hydrogen flame for excitation. The flame photometer will determine particles containing sodium, potassium and lithium down to submicron sizes, using photomultiplier detection with electronic counting and sizing which can be linked to computer evaluation.

Line reversal in atomic emission spectra is due to absorption of the characteristic emitted radiation by vapour of the element in cooler parts of the flame. The substance to be analysed by atomic absorption spectrometry is vaporized and light from a high-temperature source is passed through the vapour. The resulting absorption lines are located and identify the elements present.

The most sensitive apparatus uses, as the source of light, a hollow cathode lamp made of the element which is to be detected in the aerosol sample. A xenon lamp is employed sometimes as a continuous source; this necessitates the addition of a monochromator on the line detection side. A tunable laser has been used as a source for infrared absorption spectroscopy (Hinkley and Kelley 1971).

In order to obtain the absorption lines of elements in the sample, it has to be vaporized; the most common method of doing this, possibly after chemical processing, is to pass it into a flame. The flame section is a long, thin rectangle with the light passing through the length. An acetylene–air oxidizing flame is usual. The sample is dissolved and the solution sprayed into the mixed combustion gas in a chamber below the flame. Flameless methods of dispersing the atoms from the sample are unlikely to take over from flames in all cases, but they are steadier at low absorptions. Tin has been estimated in airborne dust collected on glass-fibre filters. A hollow tin cathode lamp was used as a source for the 2863 Å tin line. The tin was dissolved off the filter by hydrochloric acid and reacted with sodium borohydride to produce gaseous tin hydrides which were

carried by a stream of argon and freed from solid and liquid particles by impingement (Vijan and Chan 1976).

Noller and Bloom (1975) measured atmospheric lead in 200-cm^3 samples of air containing about 0·2 ng of lead.

Membrane filters were used to collect the samples which were washed with dilute nitric acid into a graphite cup whence they were vaporized and measured by atomic absorption spectrophotometry.

Flame photometric apparatus has been used for measuring very small amounts of particulate sulphur in air samples.

Flash vaporization of the deposited particles is performed by capacitor discharge, the gaseous products being carried by a stream of filtered air to the flame photometer; it has a hydrogen flame through which the gases pass. Chemiluminescence results from the formation of activated molecular sulphur and is measured with a photomultiplier tube (Lucero and Paljug 1974). Organophosphorus vapours and aerosols can be dealt with as described by Frostling (1973) and organic vapours and aerosols as described by Frostling and Brantte (1972). In these systems the electrical conductivity of the flame was measured instead of its light absorption.

Conduction is due to the presence of ions in the flame, the ion current being of the order of 10^{-5} to 10^{-3} μA. The current is not specifically related to a given compound so the system is non-discriminating. An analogous method is used in gas chromatography.

X-ray diffraction analysis of inorganic crystalline material is often limited, in applications to the study of aerosols, by the amount of material required. Originally, analysis by wavelength dispersion was effected, first by photography and then by the more sensitive proportional ionization counter. The latest development is the abandoning of wavelength dispersion in favour of energy dispersion which is measurable by solid-state counters connected to standard electronic energy sorting equipment. Elemental analysis is possible, in principle, down to atomic number 4 (Carr-Brion 1973).

An automatic computer-controlled X-ray powder diffractometer was developed by the Warren Spring Laboratory (Annual Report, 1972) which scans over a preset angular range and automatically analyses, by program, up to six diffraction maxima by means of a vertical goniometer and a proportional gas ionization counter which is driven by a stepping motor. One sample per hour is handled and the particle sizes and relative abundances of some 200 substances are read out.

Small aerosol particles, consisting of inorganic crystals, can sometimes be identified by electron diffraction. A monoenergetic beam is necessary. Owing to the short wavelength (0·04 Å at 100 kV), the angle of diffraction of the electrons by the crystal (lattice space several Å) is extremely small, but this is magnified and photographed by the imaging system of the electron microscope.

Again, in thin specimens, photoelectrons can be stimulated with monoenergetic X-rays. The emitted electrons have energies which are equal to the difference between those of the X-rays and their own binding energy. The latter depends on chemical structure. This technique has been used for sorting out the chemical states of sulphur in pollution aerosols by electron spectrometry (Craig *et al.* 1974).

The lithium-drifted silicon detector for X-rays made possible the elemental analysis of very small samples containing many elements. Development of the various ways of doing this was probably stimulated in the first place by the needs of the semiconductor industry, but there are many other fields of application and some methods are peculiarly suited to the study of aerosols.

Excitation of the emission of characteristic X-rays by the elements in the sample is achieved in several ways. In principle, they are all fluorescence processes since the sample is irradiated with particles or electromagnetic waves of wavelength shorter than those which are emitted and measured. As a rule, however, the term X-ray fluorescence is limited to systems in which excitation of the elements is caused by X-rays.

X-ray fluorescence is used for elemental analysis and is sensitive below the threshold for neutron activation. Since the characteristic X-rays are emitted immediately the stimulating radiation is received, it is possible to scan the sample and explore the distribution in it of the various elements. This was first appreciated by Coslett and Duncomb (1956) who built a scanning electron microscope with magnetic lenses and a large beam current. A particular X-ray line could be selected by means of the proportional ionization counter and used as an imaging signal.

The availability of the scanning electron microscope has encouraged the use of electron probe microanalysis (EPMA); the beam diameter is about 1 μm, so many individual aerosol particles can be examined. The X-rays excited by the electron beam are scattered in all directions. In the scanning instrument, back-scattered X-rays are analysed. With a transmission instrument (which gives better resolving power than the scanning one) it is now possible to pick up forward-scattered X-rays. This technique, transmission electron microscope microprobe analysis (EMMA), has better resolving power and can work at higher voltages, making it possible to excite the K lines of the heavier elements. It has been valuable for the identification of asbestos fibres from human lungs (Pooley 1975).

A new technique which has also been used for asbestos fibres is laser microprobe mass analysis, LAMMA (de Waele and Adams 1986). The two preceding chapters of the same book give much information about LAMMA and its application to the analysis of single aerosol particles. A 20 to 30-ns pulse is focused to a spot of 0·5 to 1·0 μm diameter and used to volatilize and partly ionize an aerosol particle which has been deposited on a cascade impactor plate; the resulting ions are analysed by a time-of-flight mass spectrometer.

Several disadvantages attach to the use of electrons to excite the characteristic X-rays of elements in a specimen of aerosol. The particles need to be of very low vapour pressure and to be stable in the electron beam so that most organic substances are ruled out. Owing to their high velocity, the electrons of the beam generate a continuous spectrum background of X-rays. The lowest concentration at which an element can be detected is of the order of 0·1%.

Considerable improvement results if the heavier protons replace electrons for inducing the emission of X-rays (PIXE). These excite X-rays at lower velocities so that the uncharacterized X-ray background is less and the limit of concentration is reduced to 0·1–1 parts per million. 2–4 MeV protons are necessary and a Van de Graaf accelerator is a suitable source.

This method of excitation was first used by Johansson *et al.* (1970). It was applied to aerosols by Axelsson *et al.* (1976), for a study of the inhalation of welding fumes.

Two five-stage cascade impactors were used, one for sampling the industrial atmosphere and the other for the air breathed out by the worker. The sampling was crude and the results show a lot of scatter. Errors vary from element to element and the detection limits are around 1 to 10 ng.

The principles and characteristics of PIXE analysis are dealt with by Traxel and Wätjen (1986) who give useful advice for its application to aerosols.

Horowitz and Grodzins (1975) were able to scan small specimens with a beam of protons giving resolution approaching 1 μm for a beam current of 100 $\mu A/m^2$. Specimens up to 10 μm thick could be analysed. Heavy ions, from high-energy accelerators, alpha particles and gamma rays from radionuclides have been used to excite X-ray emission for PIXE analysis. PIXE methods were reviewed by Birks and Gilfrich (1976).

Application to air polluting particles and interlaboratory comparisons have been discussed by Camp *et al.* (1974, 1975). Energy dispersive counting is general; automatic apparatus (Hammerle and Pierson 1975) is available for identifying sources of particulate air pollution by ratios of elements. An important result was the recognition of the Pb : Br ratio (0·25) over all particle sizes arising from leaded gasolene. (Martens *et al.* 1973).

Irradiation of particles with ions of high enough energy to cause transmutation of some of the nuclei into gamma-emitting types leads to gamma-ray dispersion analysis using a lithium-drifted germanium detector. A cyclotron was used as a source of ions for exciting lead (Desaedeleer *et al.* 1976).

When compounds, rather than elements, are the subjects of analysis the emission and absorption spectrometric methods and the X-ray emission methods can be used as detectors of gas chromatographic separation, after processing and vaporizing the sample. Mass spectrometry is also available. Electron capture detectors have been used on account of their sensitivity for many organic compounds. Lovelock and Lipsky (1960) found that trace organic vapours created characteristic reductions in the current flowing through a small ionization chamber which was activated by the thermal neutrons produced by a sealed source of alpha particles. The reduction is due to the capture of electrons by trace molecules, the electron affinity depending on specific groups in the molecule. Electron-capture detectors operate at picogram levels.

Another method for the analysis of compounds in aerosol particles is field desorption mass spectrometry which has been described by Schulten and Schurath (1975). It is suitable for substances of low volatility, including organic and inorganic salts. The source was a tungsten wire covered densely with carbonaceous needles about 30 μm long. These were loaded by impaction with the aerosol particles to be analysed. The source was fitted to the mass spectrometer which was evacuated to 10^{-5} torr. The tungsten filament was then heated in stages up to 800°C while desorption of the material proceeded; when this was complete a reference spectrum was produced by injecting a suitable vapour. From the resulting mass spectrum, ion masses were found from the positions of the lines. In a sample of the atmosphere 41 lines were seen, most of which were assigned to inorganic salts.

References

AITCHISON, J., and BROWN, J. A. C., 1963, *The Lognormal Distribution of Particle Sizes* (Cambridge University Press).

AITKEN, J., 1923, *Collected Papers*, 1839–1919, edited by C. G. Knott (Cambridge University Press).

AXELSSON, K. R., DESAEDELEER, G. G., JOHANSSON, T. B., and WINCHESTER, J. W., 1976, *Ann. occup. Hyg.*, **19**, 225.

ALTY, T., and MACKAY, C. A., 1935, *Proc. R. Soc.* A, **149**, 104–146.

ANDERSSON, F., and OLSSON, B. (eds.), 1985, *Ecol. Bull.*, **37**. An acid forest lake and its catchment (Publishing House of the Swedish Research Councils. P.O. Box 6710. S-113 85, Stockholm, Sweden).

ANYZ, F., 1966, *Tellus*, **18**, 216.

BADEMOSI, F., and LIU, B. Y. H., 1971. Publ. 155 and 156, Particle Technol. Lab. Univ. of Minnesota.
BAILEY, A. G., BALACHANDRAN, W., and WILLIAMS, T. J., 1983, *J. Aerosol Sci.*, **14**, 39–46.
BENARIE, M. M., 1981, *J. Aerosol Sci.*, **12**, 164–167.
BIGG, E. K., 1976, *J. atmos. Sci.*, **33**, 1080–1086.
BIGG, E. K., KWIZ, Z., and THOMPSON, W. J., 1971, *Tellus*, **23**, 247–259.
BIGG, E. K., and WILLIAMS, J. A., 1974, *Atmosph. Environ.*, **8**, 1.
BILLIARD, F., MADELAINE, G., and DELHAYE, J., 1970, *J. Aerosol Sci.*, **1**, 357–367.
BINEK, B., 1970, *Staub*, **30**, 468.
BINEK, B., DOHNALOVA, B., PRZYBOROWSKI, S., and ULLMANN, W., 1967, *Staub*, **27**, 379.
BIRKS, L. F., and GILFRICH, J. W., 1976, *Analyt. Chem.*, **48**, 273R.
BODHAINE, B. A., and MURPHY, M. E., 1980, *J. Aerosol Sci.*, **11**, 305–312.
BONSANG, B., NGUYEN, B. C., GAUDRY, A., and LAMBERT, G., 1981, *Atmospheric Aerosols and Nuclei*, edited by A. F. Roddy and T. C. O'Connor (Galway University Press, Ireland), pp. 508–512.
BOUCHER, R. F., and LUA, A. C., 1982, *J. Aerosol Sci.*, **13**, 499–511.
BRADLEY, R. S., EVANS, M. G., and WHYTLAW-GRAY, R. W., 1946, *Proc. R. Soc.* A, **186**, 368–384.
BRICARD, J., MADELAINE, G., and PERRON, M. L., 1981, *Atmospheric Particles and Nuclei*, edited by A. F. Roddy and T. C. O'Connor, (Galway University Press, Ireland), pp. 447–51.
BROWN, K. E., BEYER, J., and GENTRY, J. W., 1984, *J. Aerosol Sci.*, **15**, 133–145.
CALLINGHAM, M., 1980, *Int. J. cosmet. Sci.*, **2**, 107–126.
CAMP, D. C., VAN LEHN, A. L., RHODES, J. R., and PRODZINSKI, A. H., 1975, *X-Ray Spectrom.*, **4**, 123.
CAMP, D. C., COOPER, J. A., and RHODES, J. R., 1974, *X-Ray Spectrom.*, **3**, 47.
CARR-BRION, K. G., 1973, *X-Ray Spectrom.*, **2**, 63.
CARTWRIGHT, J., 1964, *Nature*, **203**, 1057.
CHEAH, P. K. P., 1983, *J. Aerosol Sci.*, **14**, 47–48.
CHEAH, P. K. P., and DAVIES, C. N., 1984, *J. Aerosol Sci.*, **15**, 741–751.
CORR, D., DOLOVICH, M., MCCORMACK, D., RUFFIN, D., OBMINSKI, G., and NEWHOUSE, M. T., 1982, *J. Aerosol Sci.*, **13**, 1–7.
CORR, D., DOLOVICH, M., OBMINSKI, G., MCCORMACK, D., and NEWHOUSE, M. T., 1983, *J. Aerosol Sci.*, **14**, 70.
COSLETT, V. E., and DUNCOMB, P., 1956, *Nature*, **177**, 1173.
CRAIG, N. L., HARKER, A. B., and NOVAKOV, T., 1974, *Atmosph. Environ.*, **8**, 15.
D'ALMEIDA, G. A., and JAENICKE, R., 1984, *J. Aerosol Sci.*, **15**, 411–413.
DAVIES, C. N., 1945, *Proc. phys. Soc.*, **57**, 259–270.
DAVIES, C. N., 1947, *Trans. Inst. Chem. Engin. Suppl.*, **25**, 25–39.
DAVIES, C. N., 1954, in *Dust is Dangerous* (London: Faber).
DAVIES, C. N., 1964, *Nature*, **201**, 172–173.
DAVIES, C. N., 1973, *Faraday Symp. Chem. Soc.* No. 7, 34–41.
DAVIES, C. N., 1974 a, *Atmosph. Environ.*, **8**, 1069–1079.
DAVIES, C. N., 1974 b, *J. Aerosol Sci.*, **5**, 293–300.
DAVIES, C. N., 1975, *J. Aerosol Sci.*, **6**, 335–347.
DAVIES, C. N., 1978, *Fundamentals of Aerosol Science*, edited by D. T. Shaw (New York: John Wiley), chap. 3.
DAVIES, C. N., 1979 a, *J. Aerosol Sci.*, **10**, 151–161.
DAVIES, C. N., 1979 b, *J. Aerosol Sci.*, **10**, 477–513.
DAVIES, C. N., 1985, *Ann. occup. Hyg.*, **29**, 13–25.
DAVIES, C. N., and AYLWARD, M., 1951, *Proc. phys. Soc.* B, **64**, 889–911.
DAVIES, C. N., and CHEAH, P. K. P., 1984, *J. Aerosol Sci.*, **15**, 719–739.
DAVIES, C. N., and EGILMEZ, N., 1985, *J. Aerosol Sci.*, **16**, 245–259.
DAVIES, C. N., and EGILMEZ, N., 1986, *Aerosol Sci. Technol.*, **5**, 117.
DAVIES, C. N., and SUBARI, M., 1982, *J. Aerosol Sci.*, **13**, 59–71.
DAVIS, E. J., and RAY, A. K., 1978, *J. Aerosol Sci.*, **9**, 411–422.
DESAEDELEER, G., RONNEAU, C., and APEOS, D., 1976, *Analyt. Chem.*, **48**, 572.
DE WAELE, J. K., and ADAMS, F. C., 1986, *Physical and Chemical Characterization of Individual Airborne Particles*, edited by K. R. Spurny (Chichester: Ellis Horwood), Chap. 15.
DYER, A. J., 1974, *Q. Jl met. Soc.*, **100**, 563–571.

EGILMEZ, N., and DAVIES, C. N., 1982, *Proc. R. Soc.* A, **380,** 99–118.
EGILMEZ, N., and DAVIES, C. N., 1984, *J. Aerosol Sci.*, **15,** 177–181.
EGILMEZ, N., and DAVIES, C. N., 1986, *Proc. Second Int. Aerosol Conf. Berlin, Sept 22–26.*
EISNER, H. S., QUINCE, B. W., and SLACK, C., 1960, *Discuss. Faraday Soc.* No. 30, 86–95.
ESMEN, N. A., ZIEGLER, P., and WHITFIELD, R., 1978, *J. Aerosol Sci.*, **9,** 547–556.
FLAGAN, R. C., and FRIEDLANDER, S. K., 1978, *Recent Developments in Aerosol Science*, edited by D. T. Shaw (New York: Wiley), Chap. 2.
FLOWERS, E. C., MCCORMICK, R. A., and KURFIS, K. R., 1969, *J. appl. Meteorol.*, **8,** 955–962.
FLYGER, H., HEIDAM, N. Z., HANSEN, K., MEGAW, W. J., WALTHER, E. G., and HOGAN, A. W., 1976, *J. Aerosol Sci.*, **7,** 103–140.
FROSTLING, H., 1973, *J. Phys.* E, **6,** 863–867.
FROSTLING, H., and BRANTTE, A., 1972, *J. Phys.* E, **5,** 251–253.
FUCHS, N., 1934, *Phys. Z. Sowjun.*, **6** (3), 224–243.
FUCHS, N., 1964, *The Mechanics of Aerosols*, edited by C. N. Davies (Oxford: Pergamon).
FUCHS, N., 1973, *J. Aerosol Sci.*, **4,** 405–410.
FUCHS, N., 1978, *Fundamentals of Aerosol Science*, edited by D. T. Shaw (New York: John Wiley), Chap. 1.
FUCHS, N. A., and SUTUGIN, A. G., 1971, High dispersed aerosols, *Topics in Current Aerosol Research*, edited by G. M. Hidy and J. R. Brock (Oxford: Pergamon).
FULWYLER, M. J., PERRINGS, J. D., and CRAM, L. S., 1973, *Rev. scient. Instrum.*, **44** (2), 204–206.
GARLAND, J. A., and BRANSON, J. R., 1977, *J. Aerosol Sci.*, **8,** 101–109.
GEBHART, J., HEYDER, J., ROTH, C., and STAHLHOFEN, W., 1980, *Staub-Reinhalt. Luft.*, **40** (1), 1–8.
GRAS, J. L., 1978, *Nature*, **271,** 231.
GRAS, J. L., 1984, *J. Aerosol Sci.*, **15,** 523–531.
GRAVENHORST, G., and MÜLLER, J., 1981, *Atmospheric Aerosols and Nuclei*, edited by A. F. Roddy and T. C. O'Connor (Galway University Press, Ireland), pp. 497–502.
GRIFFITHS, W. D., PATRICK, S., and ROOD, A. P., 1984, *J. Aerosol Sci.*, **15,** 491–502.
HAAGEN-SMIT, A. J., 1952, *Ind. Engng Chem.*, **44,** 1342–1346.
HAMMERLE, R. H., and PIERSON, W. R., 1975, *Envir. Sci. Technol.*, **9,** 1058.
HATCH, T., and CHOATE, S. P., 1929, *J. Franklin Inst.*, **207,** 369.
HEINTZENBERG, J., 1975, *J. Aerosol Sci.*, **6,** 291–303.
HINDS, W. C., 1980, *Generation of Aerosols*, edited by K. Willeke (Michigan: Ann Arbor), pp. 171–187.
HINKLEY, E. D., and KELLEY, P. L., 1971, *Science*, **171,** 635.
HODKINSON, J. R., 1966, *Aerosol Science*, edited by C. N. Davies (London and New York: Academic Press), Chap. 10.
HOGAN, A. W., and BARNARD, S., 1983, *Atmosph. Environ.*, **17,** 904.
HOGAN, A. W., BARNARD, S., MOSSL, B., and LOISEAUX, M., 1984, *J. Aerosol Sci.*, **15,** 1–12.
HOROWITZ, P., and GRODZINS, L., 1975, *Science*, **189,** 795.
INSTITUTION OF MECHANICAL ENGINEERS, 1981, *Conference of Gasborne Particles*, Oxford. 30 June–2 July. London.
ISHIZAKA, Y., and ONO, A., 1982, *Idöjaras.*, **86** (2–4), 249–253. 10th Int. Conf. Condensation Ice Nuclei. *J. Hungarian Meteorol. Service*, edited by L. Anna.
ITO, T., 1981, *Atmospheric Aerosols and Nuclei*, edited by A. F. Roddy and T. C. O'Connor (Galway University Press, Ireland), pp. 492–496.
JAENICKE, R., 1971, *J. Aerosol Sci.*, **2,** 401–404.
JAYASEKERA, P. N., and DAVIES, C. N., 1980, *J. Aerosol Sci.*, **11,** 535–547.
JEANS, J., 1925, *The Dynamical Theory of Gases* (Cambridge University Press).
JENNINGS, W., 1987, *J. Aerosol Sci.*, to be published.
JOHANSSON, T. B., AKSELSSON, R., and JOHANSSON, S. A. E., 1970, *Nucl. Instrum. Meth.*, **84,** 141.
JUNGE, C., 1963, *Air Chemistry and Radioactivity* (New York, London: Academic Press).
JUNGE, C., and MANSON, J. E., 1961, *J. geophys. Res.*, **66,** 2163–2182.
KERKER, M., 1969, *The Scattering of Light* (New York, London: Academic Press), p. 84.
KERKER, M., 1975, *Advances in Colloid and Interface Science* Volume 5, pp. 27, 105–172.
LA MER, V. K., INN, E. G. Y., and WILSON, I. B., 1950, *J. Colloid Sci.*, **5,** 471–496.
LANGER, G., and LIEBERMAN, A., 1960, *J. Colloid Sci.*, **15,** 357–360.
LEAITCH, R., and MEGAW, W. J., 1982, *J. Aerosol Sci.*, **13,** 297–319.
LEONARDO DA VINCI, 1452–1519, *Notebooks*, edited by E. MacCardy, 1948, (London: Cape), I, pp. 418–20.

LIDDELL, H. F., 1947, Porton Technical Paper No. 16.
LIDDELL, H. F., and WOOTTEN, N. W., 1957, *Q. Jl R. met. Soc.*, **83,** 263.
LIDWELL, O. M., 1946, *Nature*, **158,** 61.
LIU, B. Y. H., 1974, *APCA J.*, **24,** 1170–1171.
LIU, B. Y. H., and WHITBY, K. T., 1968, *J. Colloid Interf. Sci.*, **26,** 161–165.
LOVELOCK, J. E., and LIPSKY, R., 1960, *J. Am. chem. Soc.*, **82,** 431.
LUCERO, D. P., and PALJUG, J. W., 1974, *ASTM Spec. Tech. Publ.* No. 555 Philadelphia, Pa.
MARTENS, C. S., WESALOWSKI, J. J., KAIFER, R., and JOHN, W., 1973, *Atmosph. Environ.*, **7,** 905.
MASON, B. J., JAYARATNE, O. W., and WOODS, J. D., 1963, *J. scient. Instrum.*, **40,** 247–249.
MASUDA, H., HOCHRAINER, D., and STÖBER, W., 1979, *J. Aerosol Sci.*, **10,** 275–287.
MAY, K. R., 1945, *J. scient. Instrum.*, **22,** 187–195.
MAY, K. R., 1949, *J. appl. Phys.*, **20,** 932–938.
MAY, K. R., 1975, *J. Aerosol Sci.*, **6,** 413–419.
MAY, K. R., 1982, *J. Aerosol Sci.*, **13,** 37–47.
MEGAW, J., and WELLS, A. C., 1971, *J. Aerosol Sci.*, **2,** 161–164.
MERCHANT, J. A., BAXTER, P. *et al.*, 1982, *Inhaled Particles V*, edited by W. H. Walton (Oxford: Pergamon), pp. 911–9.
MILLER, S. W., and BODHAINE, B. A., 1982, *J. Aerosol Sci.*, **13,** 481–490.
MINAERT, M., 1954, *Light and Colour in the Open Air* (New York: Dover), Chap. 10.
MOKLER, B. V., WONG, B. A., and SNOW, J., 1979, *Am. ind. Hyg. Ass. J.*, **40,** 330–347.
MÖLLER, D., 1984, *Atmosph. Environ.*, **18,** 19–27; 29–39.
MORALES, C. (ed.), 1979, *Scope 14, Sahara dust* (Chichester: John Wiley).
MUIR, D. C. F., 1965, *Ann. occup. Hyg.*, **8,** 233–238.
NARUSAWA, U., and SPRINGER, G. S., 1975, *J. Colloid Interf. Sci.*, **50,** 392–395.
NEWMAN, S. P., 1983, *J. Aerosol Sci.*, **14,** 69.
NOLAN, P. J., 1972, *Sci. Proc. R. Dublin Soc.*, **4** (12), 161–180.
NOLAN, P. J., and POLLAK, L. W., 1946, *Proc. R. Irish Acad.*, **51** (A2), 9–31.
NOLLER, B. N., and BLOOM, H., 1975, *Atmosph. Environ.*, **9,** 805.
ORR, C., HURD, F. K., and CORBETT, W. J., 1958, *J. Colloid Sci.*, **13,** 472–482.
PADMA, D. V., NAIR, P. V. N., and VOHRA, K. G., 1984, *J. Aerosol Sci.*, **15,** 553–561.
PAUL, B., 1961, *ARS J.*, **32,** 1321–3128.
PAW, U. K. T., 1983, *J. Colloid Interf. Sci.*, **93,** 442–452.
PENGILLY, R. W., and KEINER, J. A., 1977, *J. Soc. cosmet. Chem.*, **28,** 641–650.
POLLAK, L. W., 1959, *Int J. Air Pollut.*, **1,** 293–306.
POLLAK, L. W., and METNIEKS, A. L., 1960, Tech. Sci. Note No. 9. School of Cosmic Physics, Dublin Institute for Advanced Studies.
POOLEY, F. D., 1975, *Ann. occup. Hyg.*, **18,** 181.
PRODI, F., and TOMASI, C., 1983, *J. Aerosol Sci.*, **14,** 517–527.
RAABE, O. G., 1968, *Am. ind. Hyg. Ass. J.*, **29,** 439–443.
RENOUX, A., PAUGAM, J-Y., MADELAINE, G., and FOUGANG, S., 1981, *Atmospheric Aerosol and Nuclei*, edited by A. F. Roddy and T. C. O'Connor (Galway University Press, Ireland), pp. 512–517.
ROBINSON, E., and ROBBINS, R. C., 1971, Stanford Research Institute Final Report of SRI Project SCC-8507.
RODDY, A. F., and O'CONNOR, T. C. (eds.), 1981, *Atmospheric Aerosols and Nuclei* (Galway University Press, Ireland).
ROOKER, S. J., and DAVIES, C. N., 1979, *J. Aerosol Sci.*, **10,** 139–150.
ROSIN, P., and RAMMLER, E., 1933, *J. Inst. Fuel*, **7,** 2–36.
SANDBERG, D. V., PIEROVICH, J. M., FOX, D. V., and ROSS, E. W., 1979, Effects of fire on air. First Series. U.S. Dept. of Agriculture General Tech. Rep. WO-9.
SCHEIBEL, H. G., and PORSTENDORFER, J., 1984, *J. Aerosol Sci.*, **15,** 673–682.
SCHMITT, J. L., KASSNER, J. L., and PODZIMEK, J., 1982, *J. Aerosol Sci.*, **13,** 373–389.
SCHULTEN, H.-R., and SCHURATH, U., 1975, *Atmosph. Environ.*, **9,** 1107–1112.
SHAW, G. E., 1976, *Science*, **192,** 1334–1336.
SINCLAIR, D., 1984, *Aerosol Sci. Technol.*, **3,** 125–134.
SINCLAIR, D., and KNUTSON, E. O., 1986, *Aerosol Sci. Technol.*, **5,** 119–120.
SINCLAIR, D., and LA MER, V. K., 1949, *Chem. Rev.*, **44,** 245.
SKINNER, L. M., and SAMBLES, J. R., 1972, *J. Aerosol Sci.*, **3,** 199–210.

SMITH, W. H., 1981, *Air Pollution and Forests* (New York, Berlin: Springer).
SMOLUCHOWSKI, M. VON, 1917, *Z. Phys. Chem.*, **92,** 129–191.
SPURNY, K., 1981, *Staub-Reinhalt Luft.*, **41,** 330–335.
SPURNY, K. (ed.), 1986, *Physical and Chemical Characterization of Individual Airborne Particles* (Chichester: Ellis Horwood).
STAHLHOFEN, W., GEBHART, J., HEYDER, J., and ROTH, C., 1975, *J. Aerosol Sci.*, **6,** 161–167.
SUZUKI, T., SWIFT, D. L., WAGNER, H. N., and PROCTER, D. F., 1982, *Europ. J. nucl. Med.*, **7,** 474–479.
SWIFT, D. L., 1967, *Ann. occup. Hyg.*, **10,** 337–348.
TANAKA, I., and AKIYAMA, T., 1984, *Aerosols*, edited by B. Y. H. Liu and H. J. Fissan (New York: Elsevier), pp. 701–4.
TANG, I. N., 1976, *J. Aerosol Sci.*, **7,** 361–371.
TARRONI, G., 1971, *J. Aerosol Sci.*, **2,** 257–260.
TOMASI, C., VITALE, V., and EZIO, C., 1983, *J. Aerosol Sci.*, **14,** 529–539.
TRAXEL, K., and WÄTJEN, U., 1986, *Physical and Chemical Characterization of Individual Airborne Particles*, edited by K. R. Spurny (Chichester: Ellis Horwood), Chap. 16.
TURCO, R. P., TOON, O. B., ACKERMAN, T. P., POLLACK, J. B., and SAGAN, S., 1983, *Science*, **222,** 1283–1292.
TURCO, R. P., TOON, O. B., ACKERMAN, T. P., POLLACK, J. B., and SAGAN, S., 1984, *Scient. Am.*, **251,** 23–33.
VIJAN, P. N., and CHAN, C. Y., 1976, *Analyt. Chem.*, **48,** 1788.
WALLER, R. E., 1963, *Int. J. Air Water Pollution*, **7,** 773.
WALTON, W. H., and PREWETT, W. C., 1949, *Proc. phys. Soc.* B, **62,** 341–350.
WIEGNER, G., 1911, *Kolloidzeitschrift*, **8,** 227.
WILKINSON, M. C., MATTISON, I. C., and COX, R. A., 1974, Unclassified Porton Technical Paper No. 139. CDE, Porton Down, Salisbury, Wilts.
WILLEKE, K., LO, C. S. K., and WHITBY, K. T., 1974, *J. Aerosol Sci.*, **5,** 449–455.
WINKLER, P., 1973, *J. Aerosol Sci.*, **4,** 373–387.
WINKLER, P., 1974, *J. Aerosol Sci.*, **5,** 235–240.
WRIGHT, P. G., 1960, *Discuss Faraday Soc.*, **30,** 100.
ZEBEL, G., 1956, *Z. Aerosol-Forsch. u. Ther.*, **5,** 263–288.